

Electronic Supplementary Information

**Effect of Substitution on Halide/Hydrated Halide
Binding: A Case Study of Neutral Bis Urea
Receptors**

*Asesh Das, Biswajit Nayak and Gopal Das**

Department of Chemistry, Indian Institute of Technology Guwahati,

Assam-781039, India

E-mail: gdas@iitg.ac.in

Table of Contents

¹ H-NMR spectrum (full as well as expanded) of Chloride complex of L ₁	Figure S1
FT-IR spectrum of Chloride complex of receptor L ₁	Figure S2
¹ H-NMR spectrum (full as well as expanded) of Bromide complex of L ₁	Figure S3
FT-IR spectrum of Bromide complex of receptor L ₁	Figure S4
¹ H-NMR spectrum (full as well as expanded) of free receptor L ₂	Figure S5
FT-IR spectrum of receptor L ₂	Figure S6
ESI-Mass spectrum of dipodal receptor L ₂	Figure S7
¹ H-NMR spectrum (full as well as expanded) of Chloride complex of L ₂	Figure S8
FT-IR spectrum of Chloride complex of receptor L ₂	Figure S9
¹ H-NMR spectrum (full as well as expanded) of Bromide complex of L ₂	Figure S10
FT-IR spectrum of Bromide complex of receptor L ₂	Figure S11
¹ H-NMR spectrum (full as well as expanded) of free receptor L ₃	Figure S12
ESI-Mass spectrum of dipodal receptor L ₃ .	Figure S13
FT-IR spectrum of receptor L ₃ recorded	Figure S14
¹ H-NMR spectrum (full as well as expanded) of Chloride complex of L ₃	Figure S15
FT-IR spectrum of Chloride complex of receptor L ₃	Figure S16
¹ H-NMR spectrum (full as well as expanded) of Bromide complex of L ₃	Figure S17
FT-IR spectrum of Bromide complex of receptor L ₃	Figure S18
¹ H-NMR spectrum (full as well as expanded) of free receptor L ₄	Figure S19
ESI-Mass spectrum of dipodal receptor L ₄ .	Figure S20
FT-IR spectrum of receptor L ₄ recorded	Figure S21
¹ H-NMR spectrum (full as well as expanded) of Chloride complex of L ₄	Figure S22
FT-IR spectrum of chloride complex of receptor L ₄	Figure S23
¹ H-NMR spectrum (full as well as expanded) Bromide complex of receptor L ₄	Figure S24
FT-IR spectrum of Bromide complex of dipodal receptor L ₄	Figure S25
X-ray structure analysis of complex 1a showing coordination environment of anion as well as extra stabilization through C-H _{aliphatic} ...O _{urea} and C-H _{aliphatic} ... π _{aromatic} interaction with proper bond distances in Angstrom.	Figure S26
X-ray structure analysis of complex 1b showing coordination environment of anion as well as extra stabilization through C-H _{aliphatic} ...O _{urea} , C-H _{aliphatic} ... π _{aromatic} C-H _{aliphatic} ...O _{water} interaction with proper bond distances in Angstrom.	Figure S27
X-ray structure analysis of complex 2a showing coordination environment of anion as well as extra stabilization through two C-H _{aliphatic} ...O _{urea} with proper bond distances in Angstrom.	Figure S28
X-ray structure analysis of complex 2b showing coordination environment of anion as well as extra stabilization through C-H _{aliphatic} ...O _{urea} , with proper bond distances in Angstrom.	Figure S29
X-ray structure analysis of complex 3a showing coordination environment of anion as well as extra stabilization through three C-H _{aliphatic} ...O _{urea} , four C-H _{aliphatic} ...O interaction.	Figure S30
X-ray structure analysis of complex 3b showing coordination environment of anion as well as extra stabilization through three C-H _{aliphatic} ...O _{urea} , two C-H	Figure S31

aliphatic...O interaction involving one oxygen atom of substituted NO ₂ group with proper bond distances in Angstrom.	
X-ray structure analysis of complex 4a showing coordination environment of anion as well as extra stabilization through two C-H _{aliphatic} ...O _{urea} interaction with proper distances in Angstrom.	Figure S32
X-ray structure analysis of complex 4b showing coordination environment of anion as well as extra stabilization through three C-H _{aliphatic} ...O _{urea} interaction with proper distances in Angstrom.	Figure S33
The scatter plot of N-H...A angle vs. H...A distance of the hydrogen bonds in the complexes (1a , 1b , 2a , 2b , 3a , 3b , 4a and 4b).	Figure S34
¹ H NMR titration plot and bind-fit curve of Chloride complex of L₁	Figure S35
¹ H NMR titration plot and bind-fit curve of Bromide complex of L₁	Figure S36
¹ H NMR titration plot and bind-fit curve of Chloride complex of L₂	Figure S37
¹ H NMR titration plot and bind-fit curve of Bromide complex of L₂	Figure S38
Hydrogen bonding distances (Å) and Bond angles (°) in the neutral anion-receptor complexes.	Table S1
Contact contributions from the d _{norm.} surface areas of dipodal segments in free receptors and in anion complexes.	Table S2

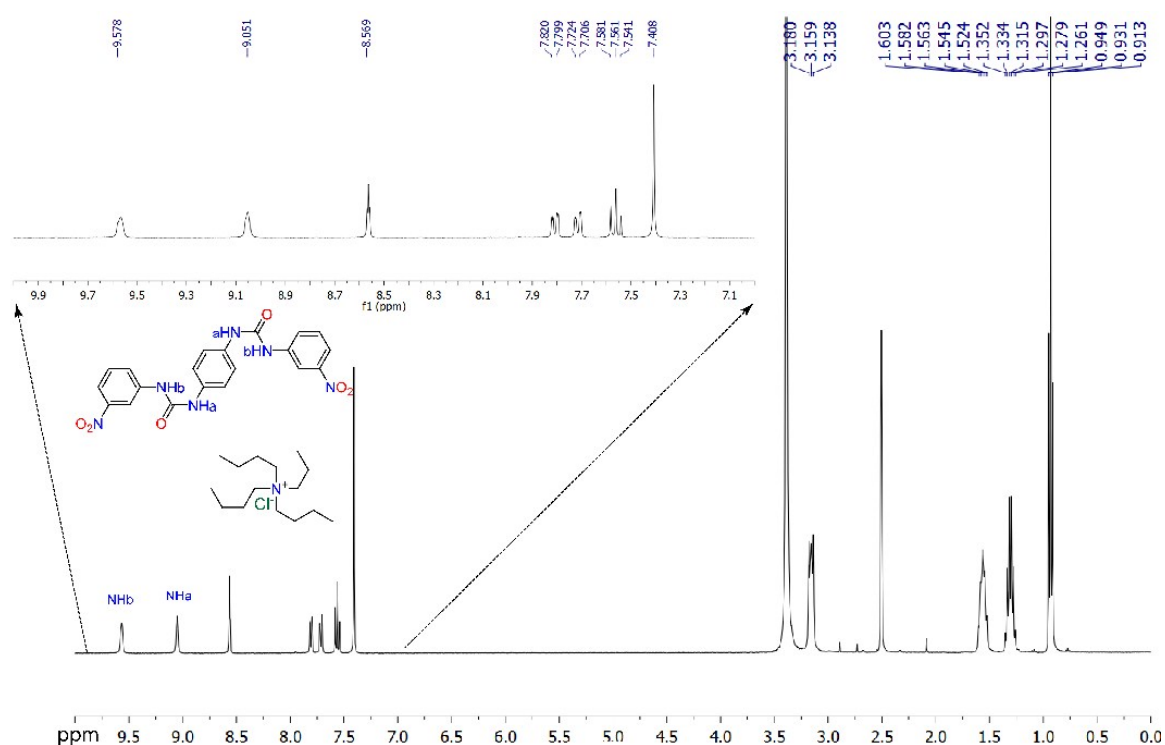


Figure S1: Integrated ¹H-NMR spectrum (full as well as expanded) of Chloride complex of **L₁** in DMSO-d₆ at 25°C.

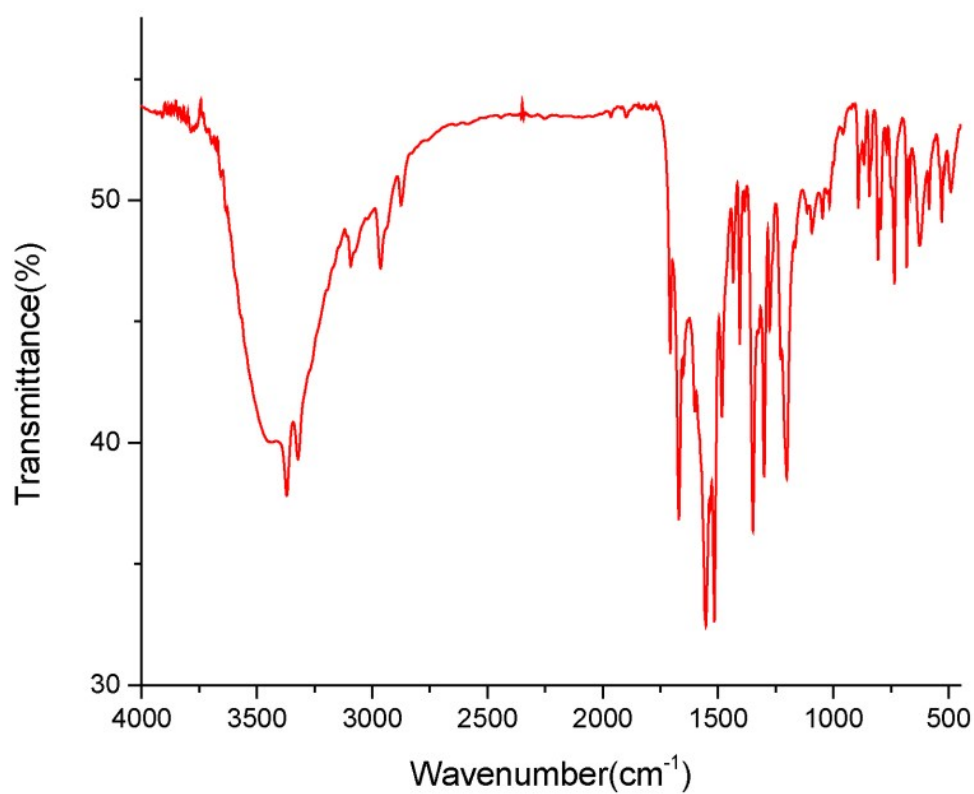


Figure S2: FT-IR spectrum of Chloride complex of receptor **L**₁ recorded in KBr pellet.

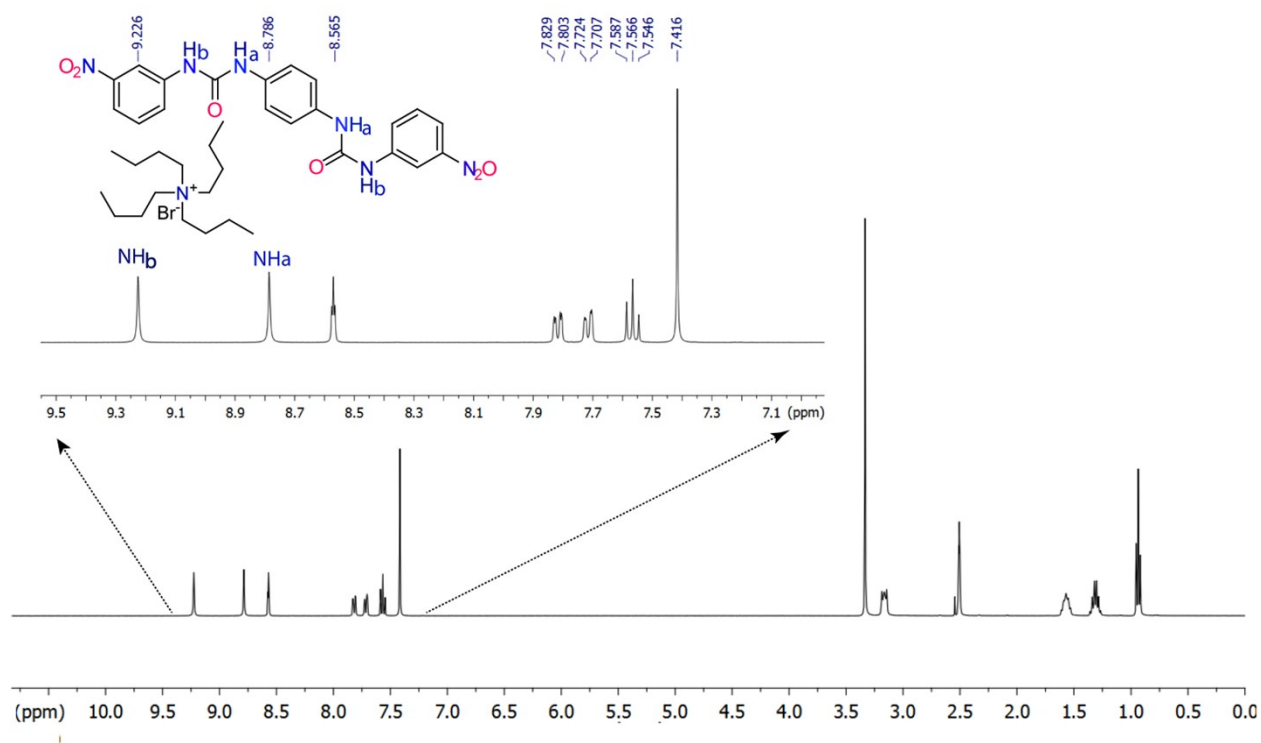


Figure S3: Integrated ¹H-NMR spectrum (full as well as expanded) of Bromide complex of **L**₁ in DMSO-d₆ at 25°C.

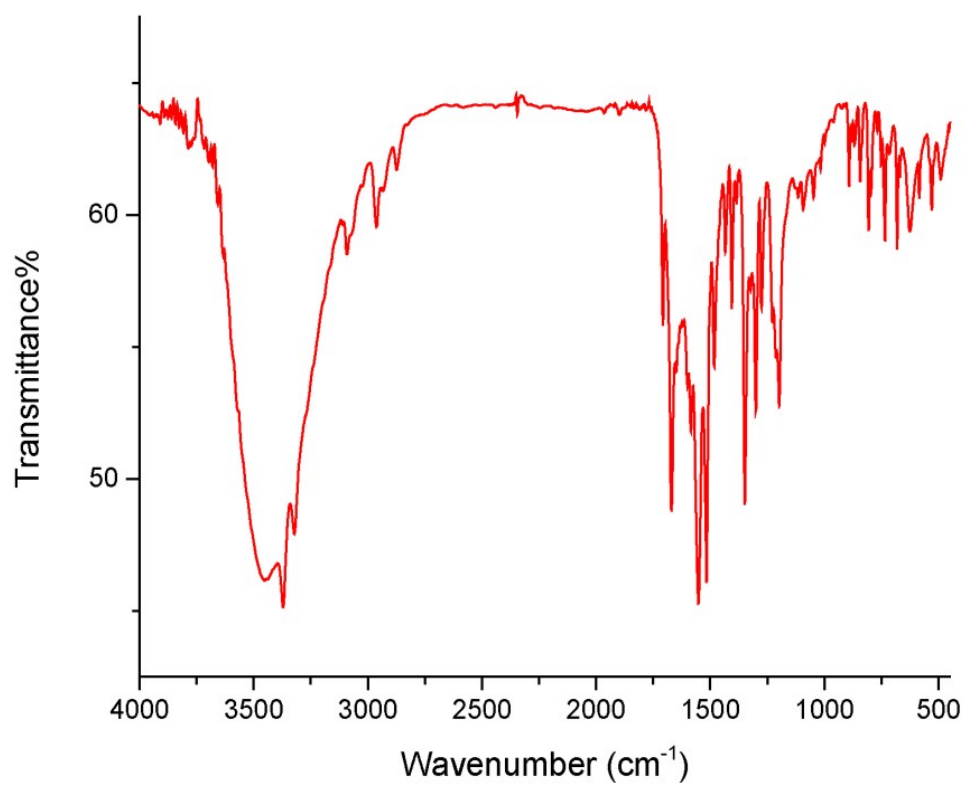


Figure S4: FT-IR spectrum of Bromide complex of receptor **L₁** recorded in KBr pellet.

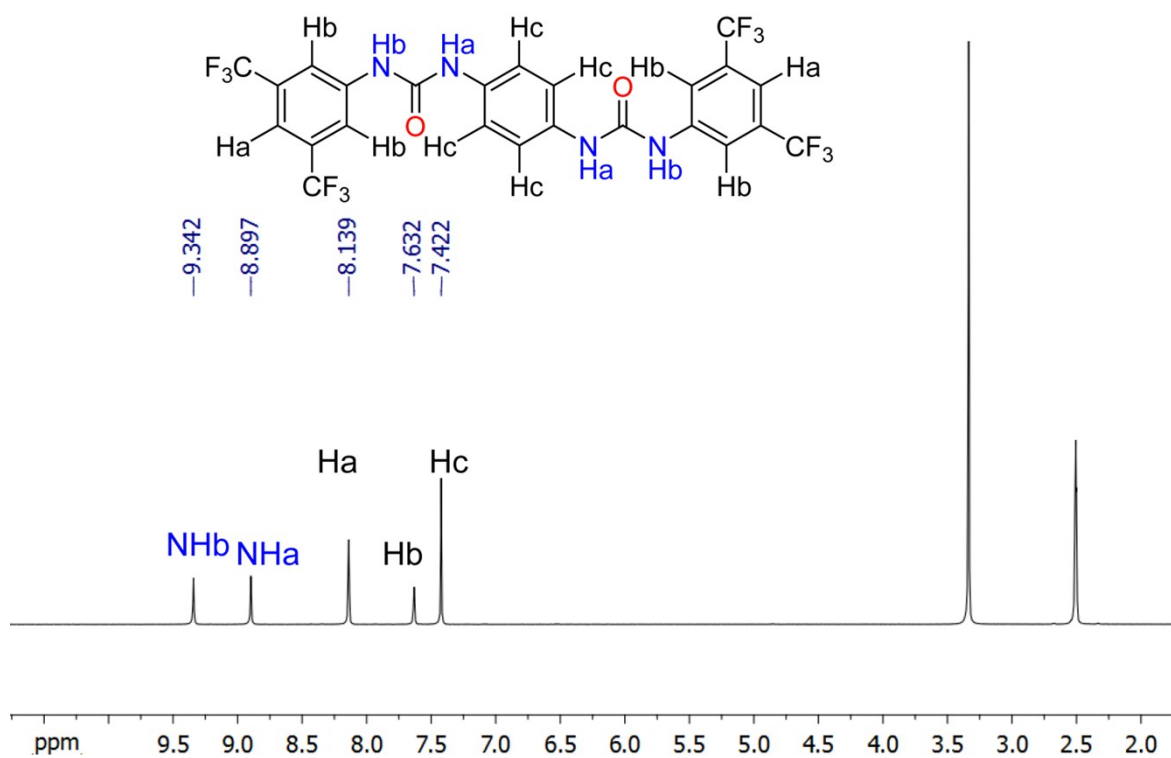


Figure S5: Integrated ^1H -NMR spectrum (full as well as expanded) and explanation of all hydrogen atoms of free dipodal receptor L_2 in DMSO-d_6 at 25°C .

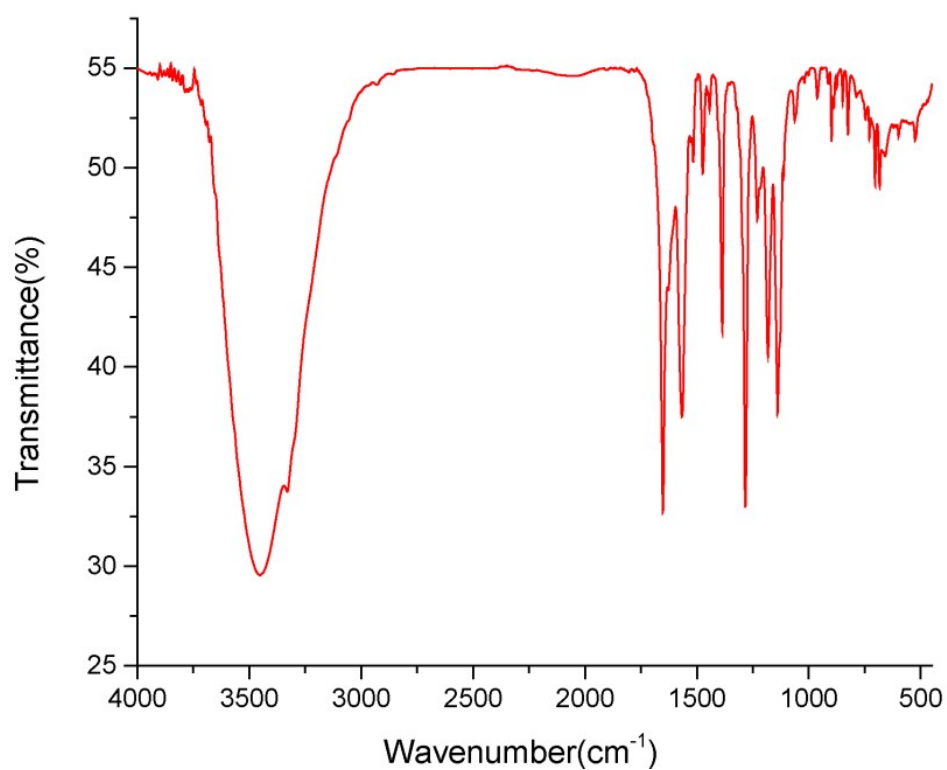


Figure S6: FT-IR spectrum of receptor L_2 recorded in KBr pellet.

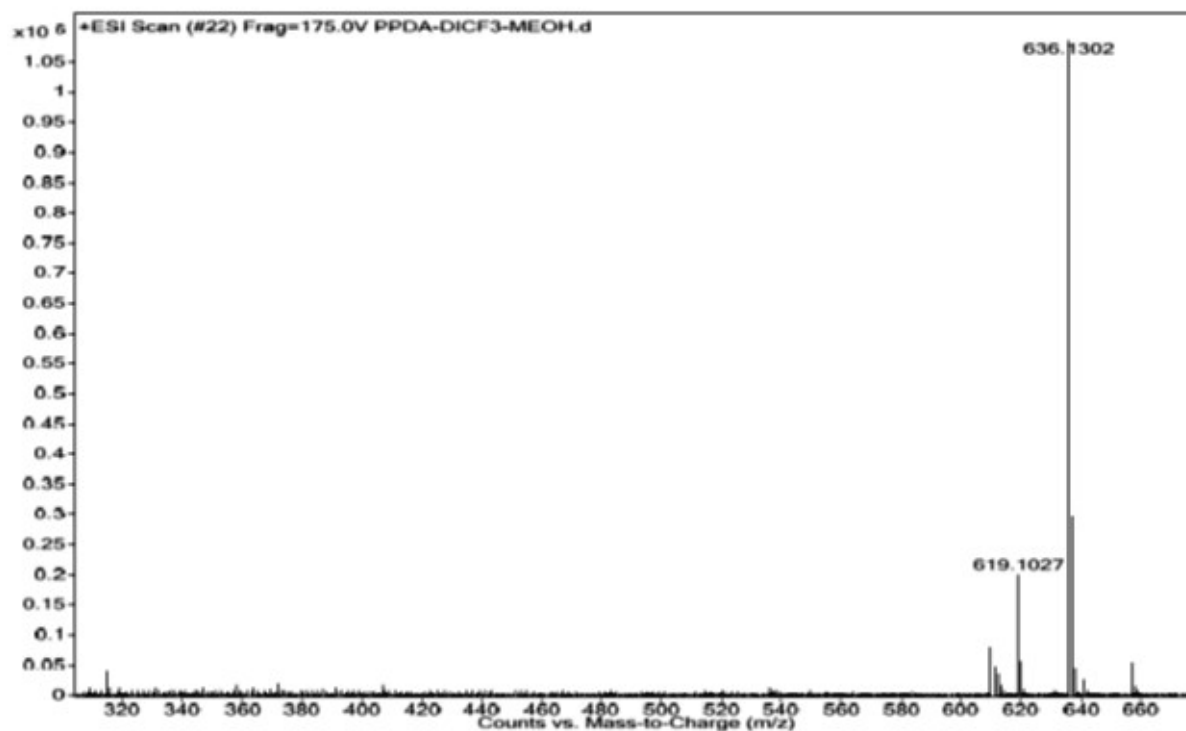


Figure S7: ESI-Mass spectrum of dipodal receptor **L**₂.

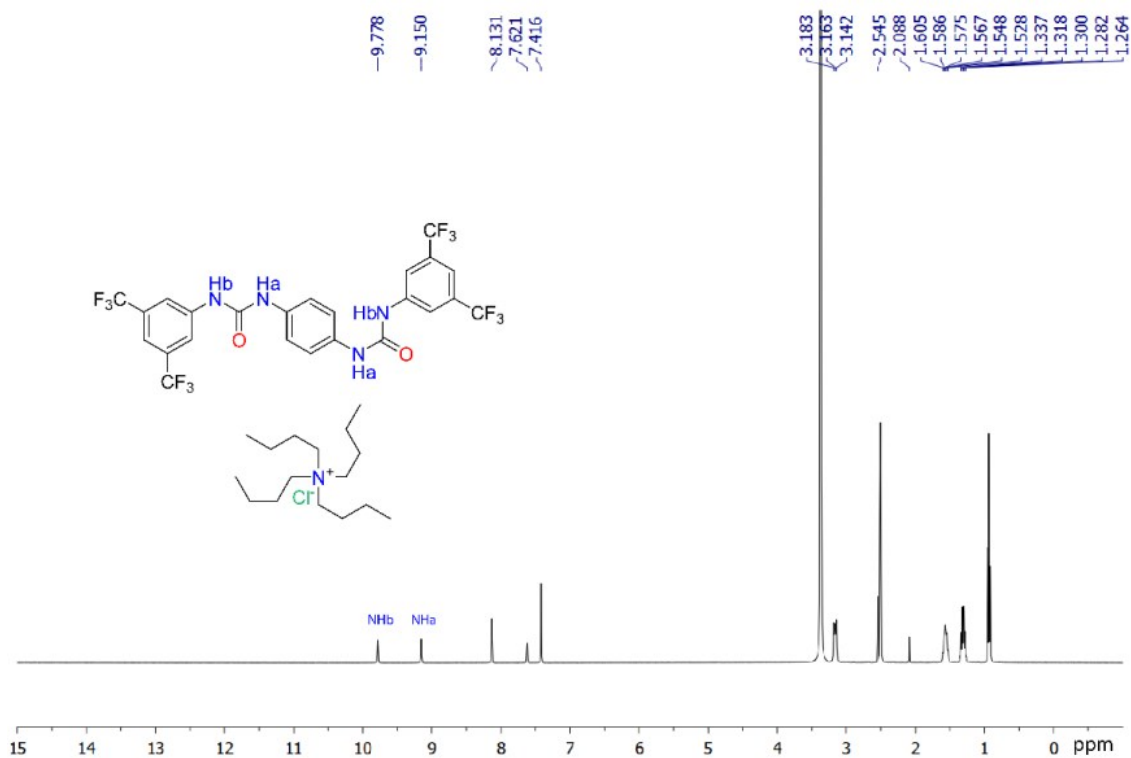


Figure S8: Integrated ¹H-NMR spectrum (full as well as expanded) of Chloride complex of receptor **L**₂ in DMSO-d₆ at 25°C.

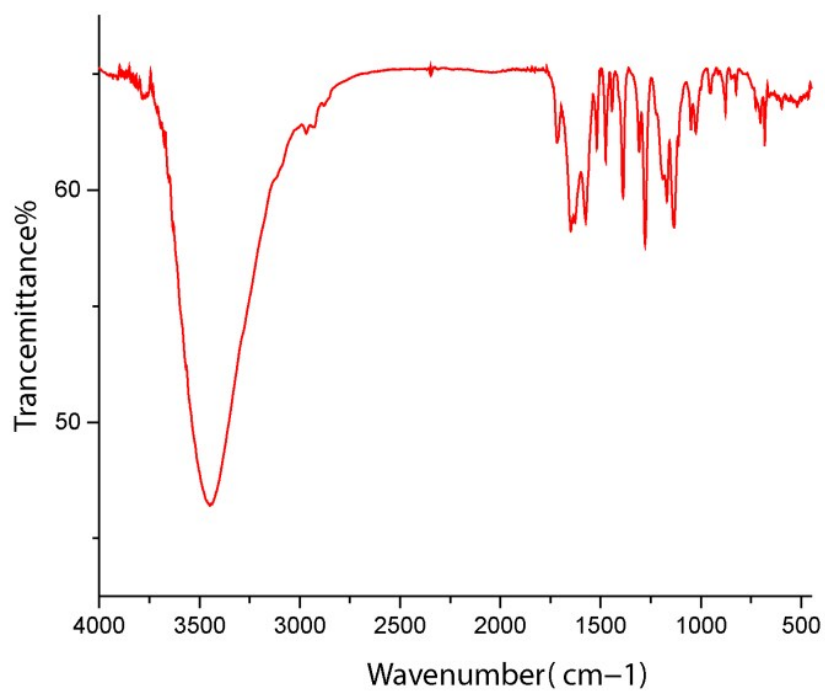


Figure S9: FT-IR spectrum of Chloride complex of receptor **L**₂ recorded in KBr pellet.

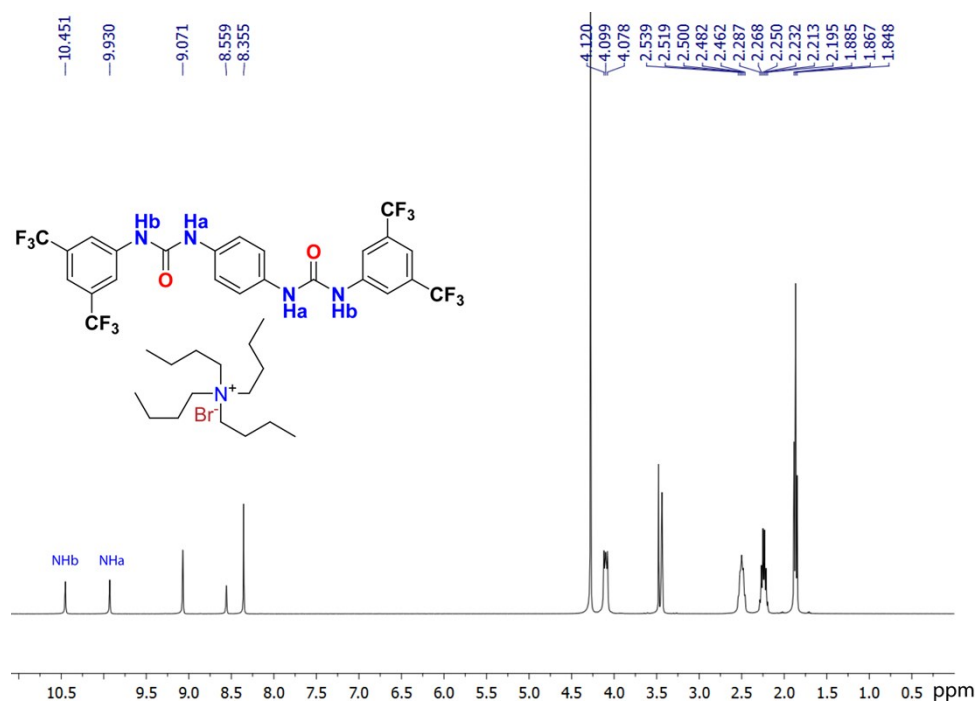


Figure S10: Integrated 1H -NMR spectrum (full as well as expanded) of Bromide complex of receptor L_2 in $DMSO-d_6$ at $25^\circ C$.

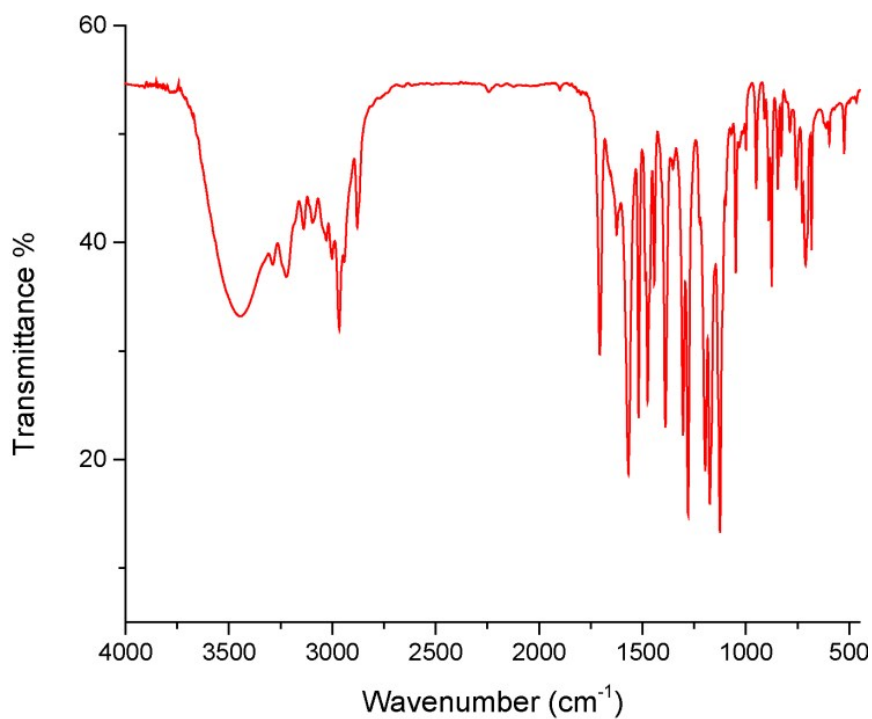


Figure S11: FT-IR spectrum of Bromide complex of receptor L_2 recorded in KBr pellet.

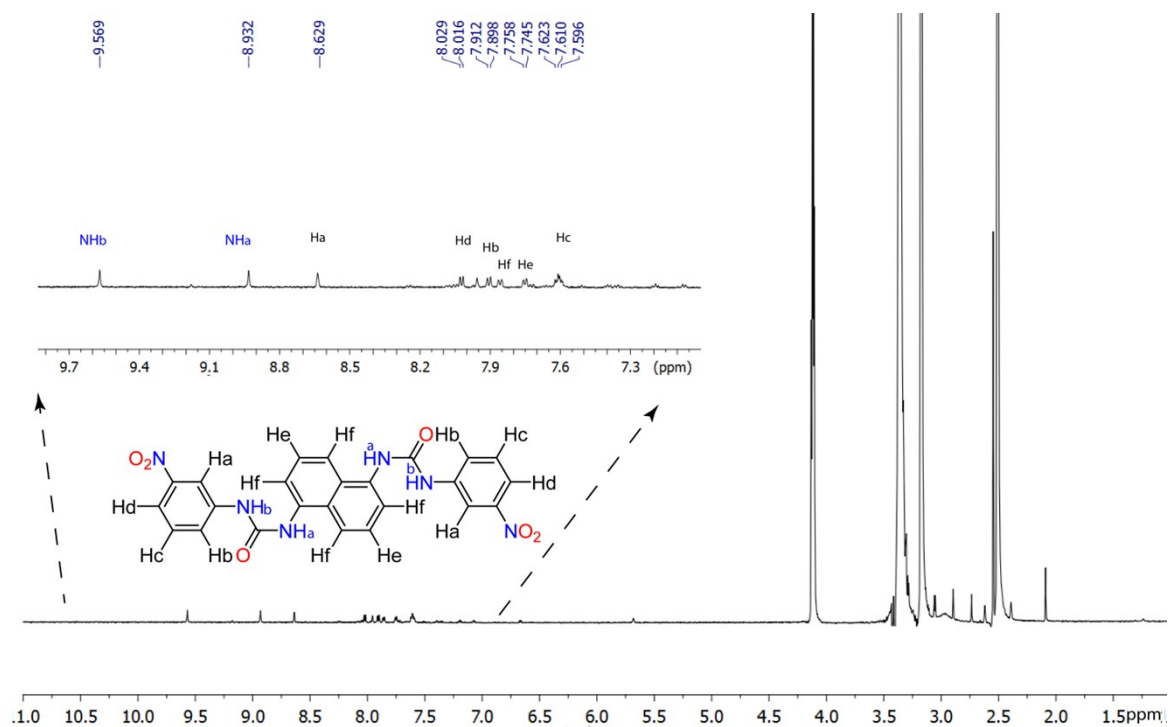


Figure S12: Integrated ^1H -NMR spectrum (full as well as expanded) and explanation of all hydrogen atoms of free dipodal bis-urea receptor L_3 in DMSO-d_6 at 25°C .

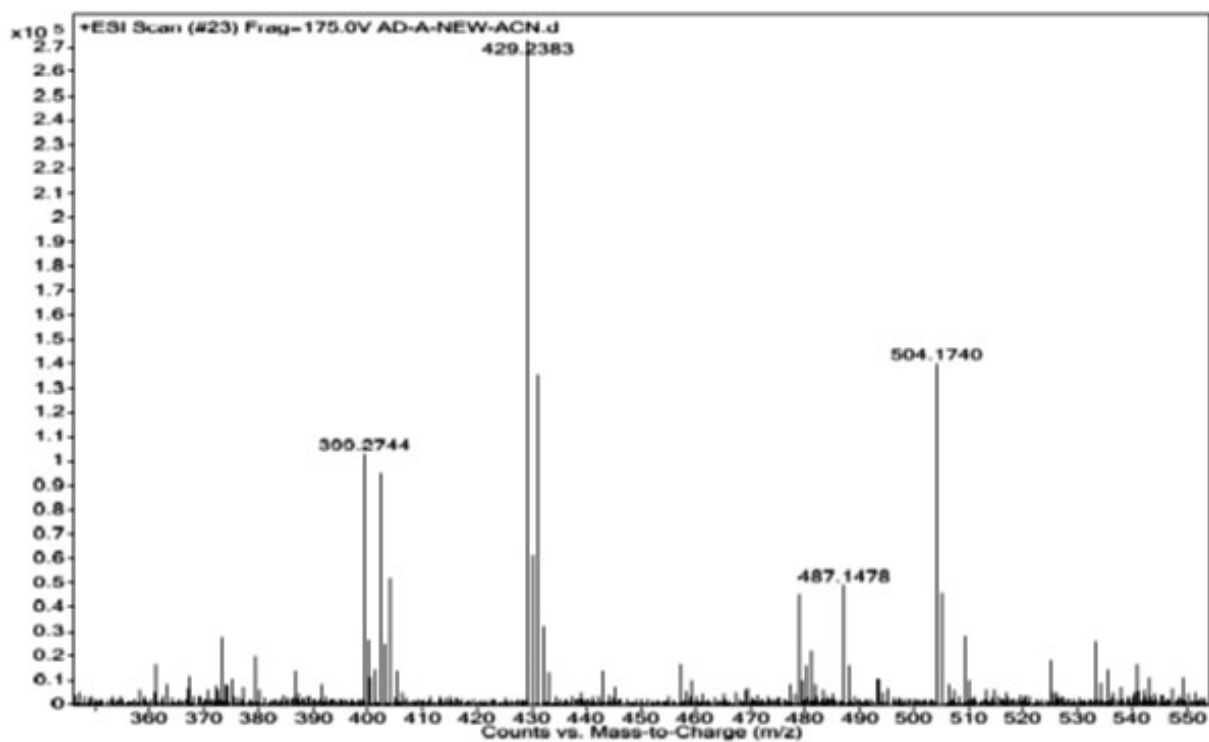


Figure S13: ESI-Mass spectrum of dipodal receptor L_3 .

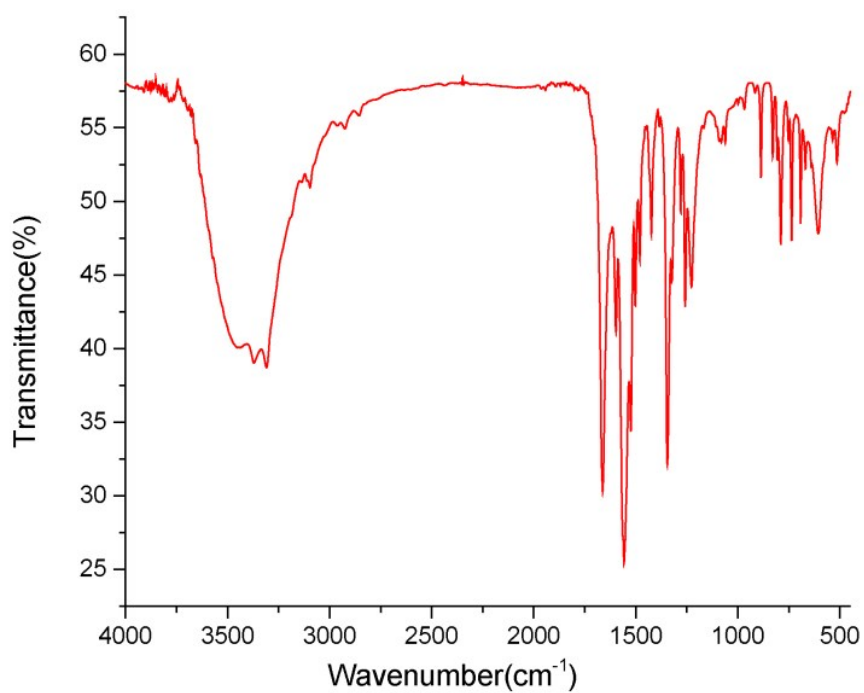


Figure S14: FT-IR spectrum of receptor **L**₃ recorded in KBr pellet.

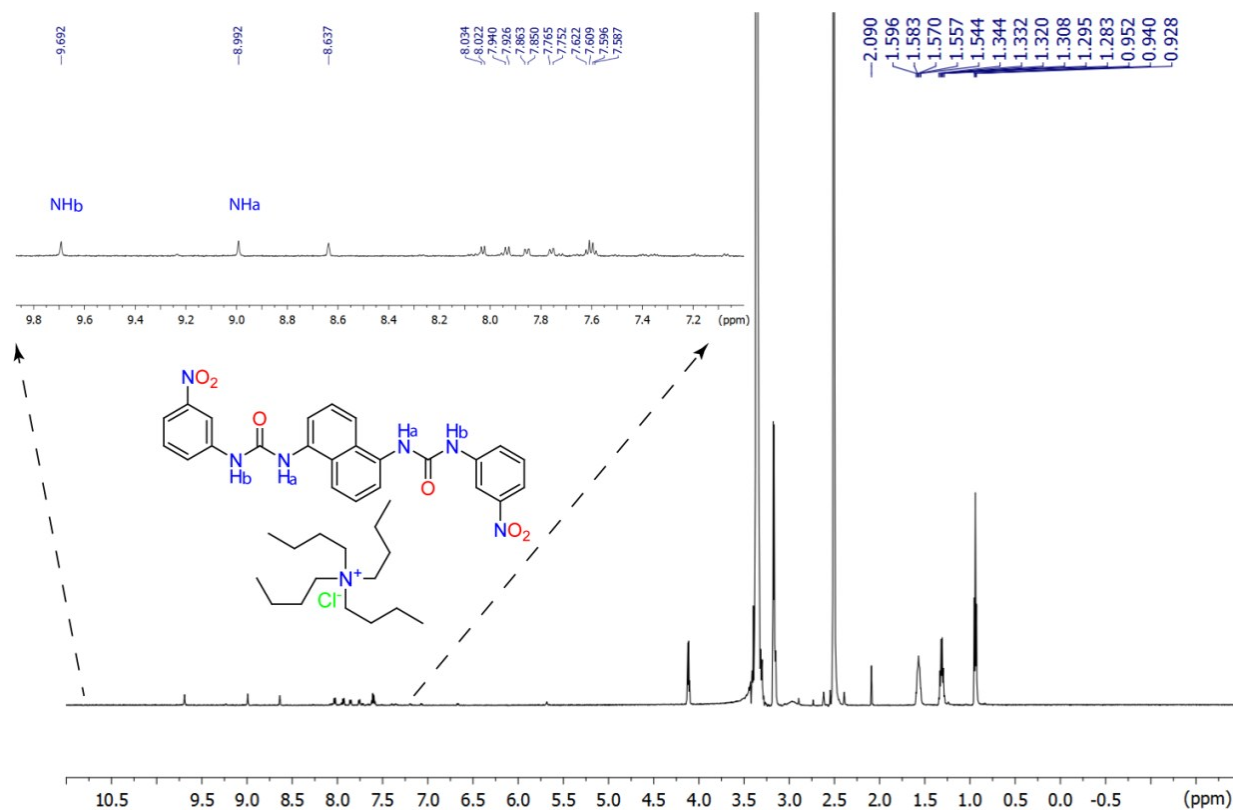


Figure S15: Integrated ¹H-NMR spectrum (full as well as expanded) of Chloride complex of receptor **L**₃ in DMSO-*d*₆ at 25°C.

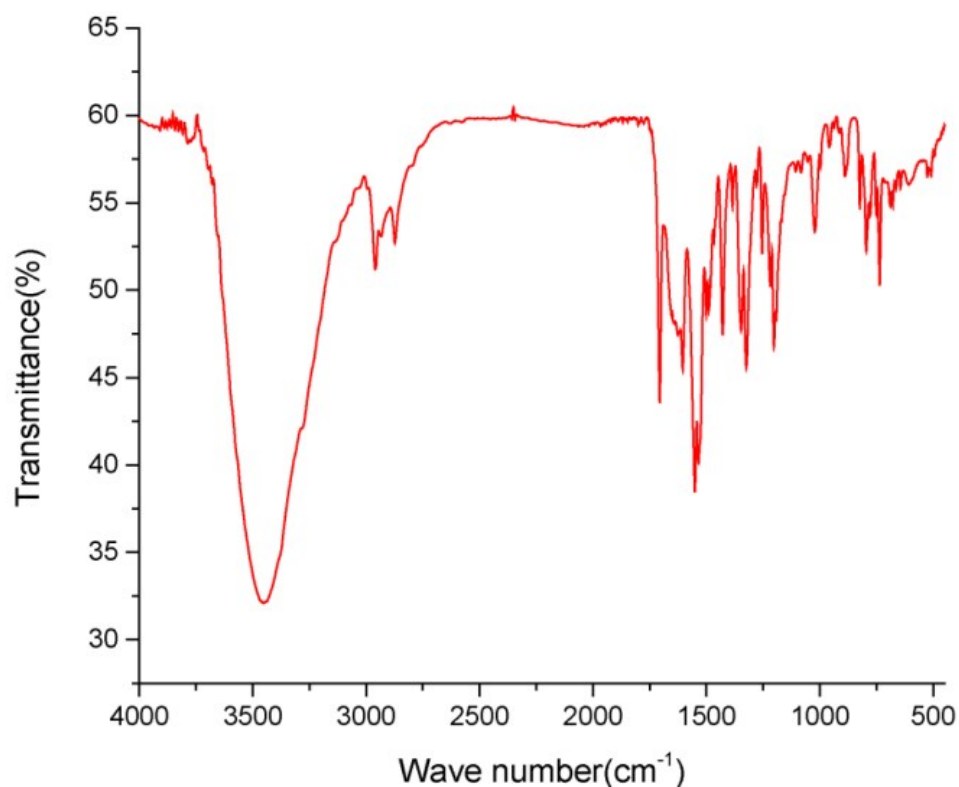


Figure S16: FT-IR spectrum of Chloride complex of receptor **L**₃ recorded in KBr pellet.

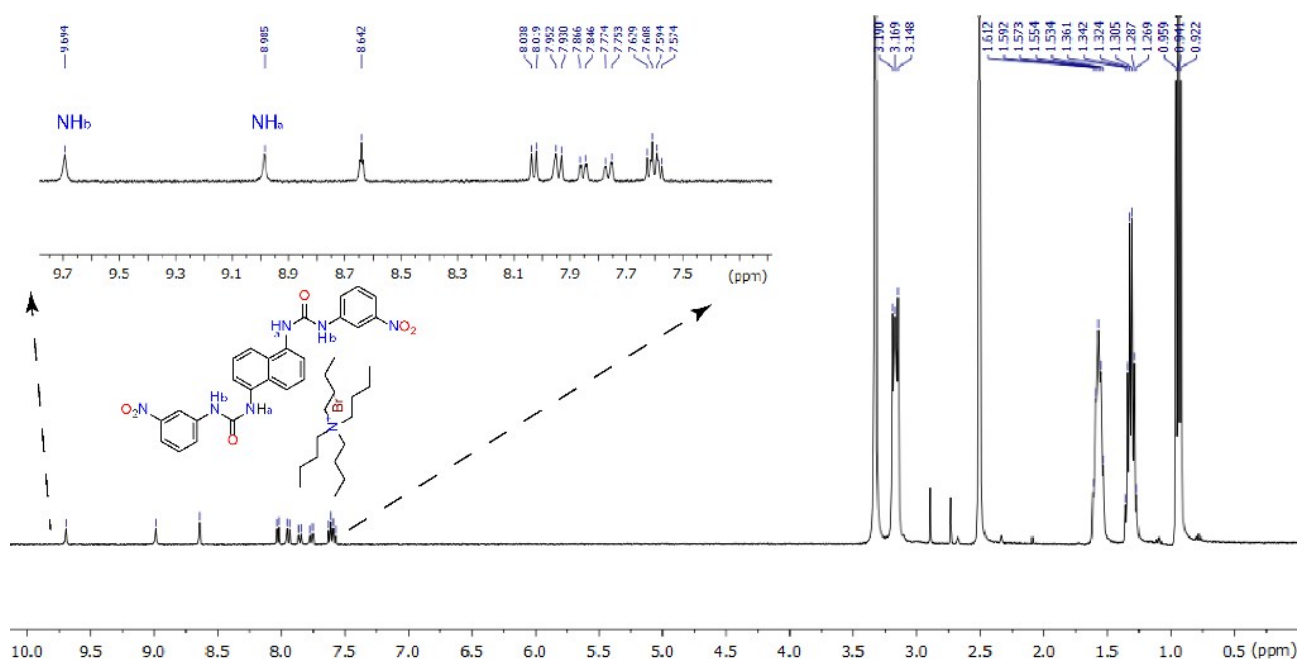


Figure S17: Integrated ¹H-NMR spectrum (full as well as expanded) of Bromide complex of receptor **L**₃ in DMSO-*d*₆ at 25°C.

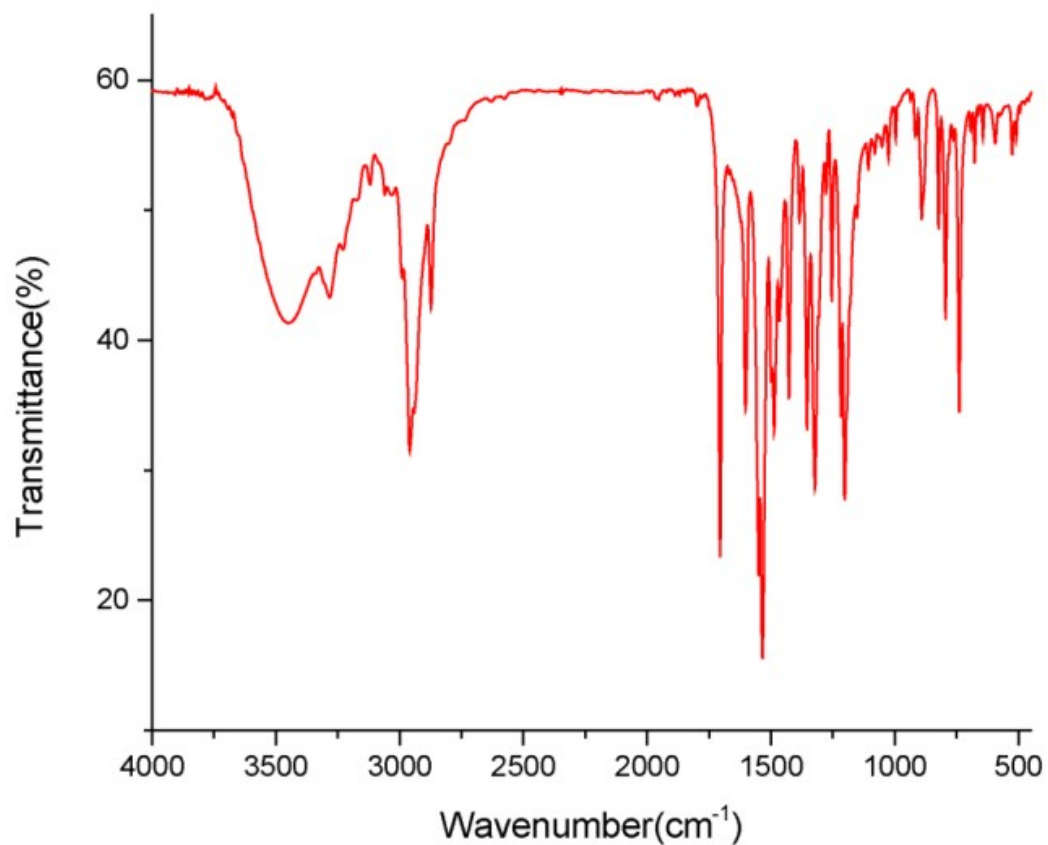


Figure S18: FT-IR spectrum of Bromide complex of receptor **L**₃ recorded in KBr pellet.

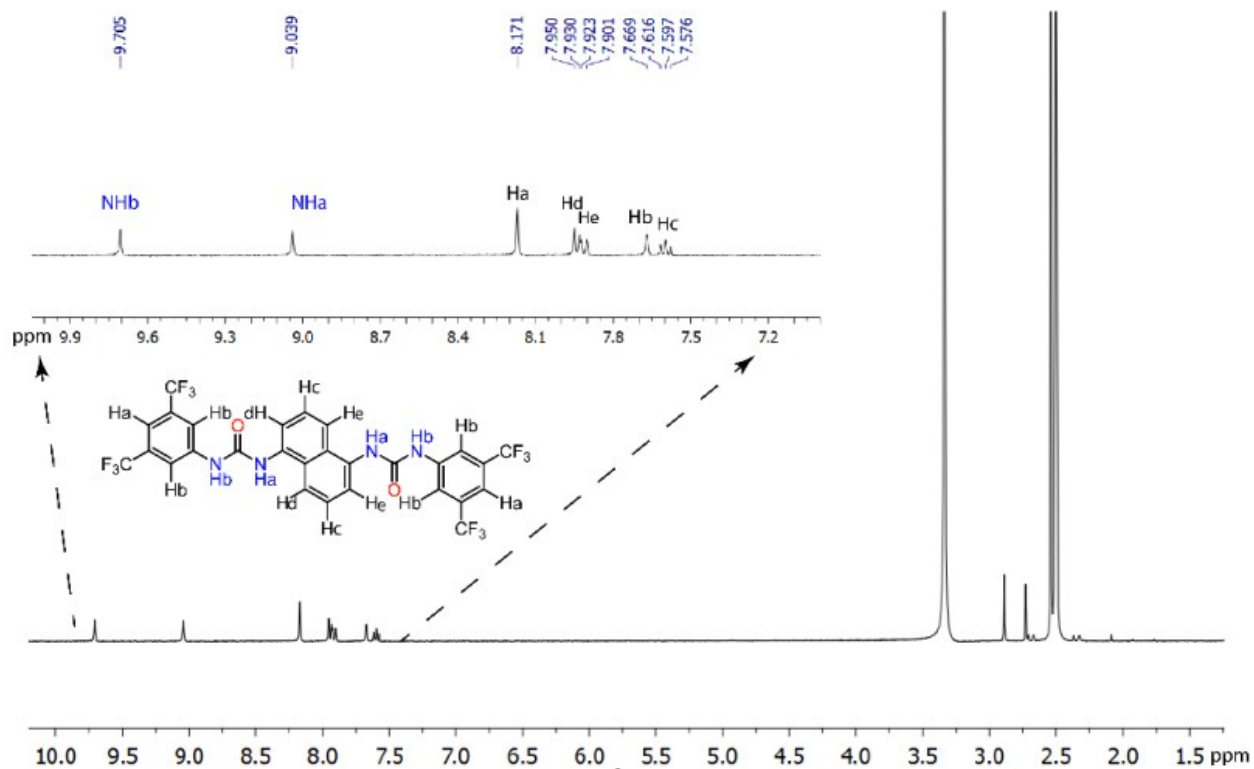


Figure S19: Integrated ¹H-NMR spectrum (full as well as expanded) and explanation of all hydrogen atoms of free dipodal bis urea receptor **L**₄ in DMSO-*d*₆ at 25°C.

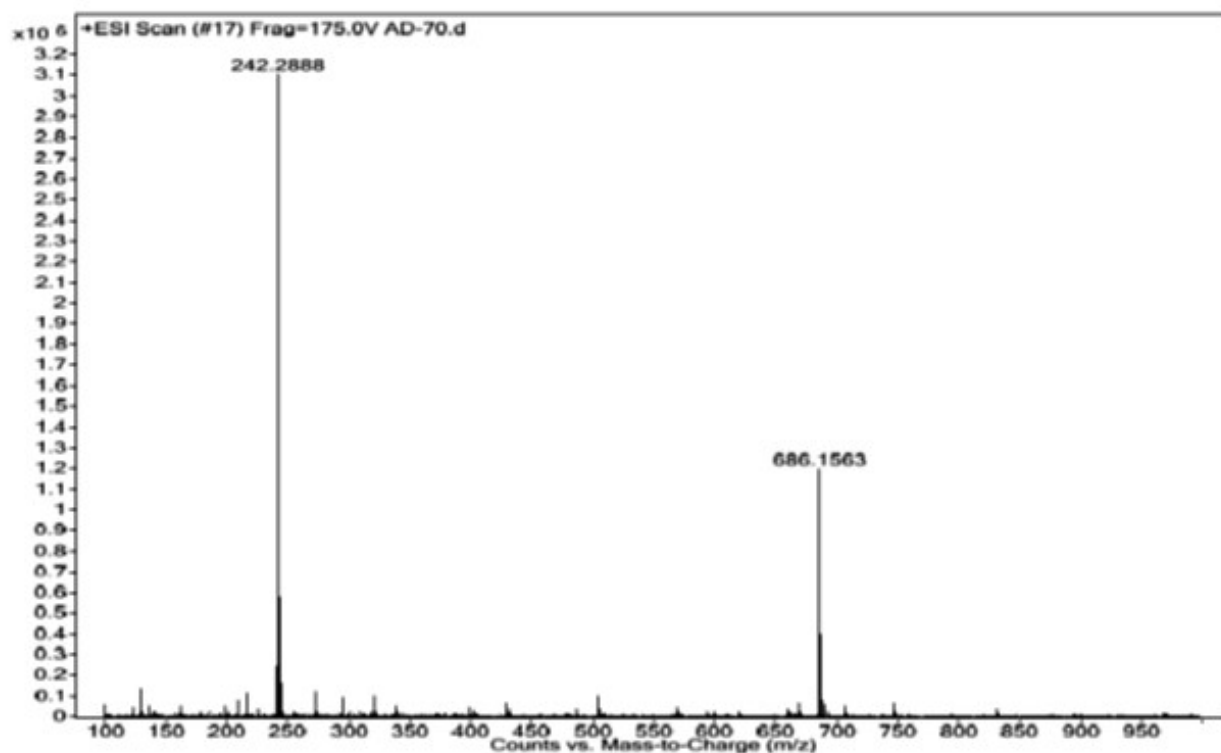


Figure S20: ESI-Mass spectrum of dipodal receptor **L₄**.

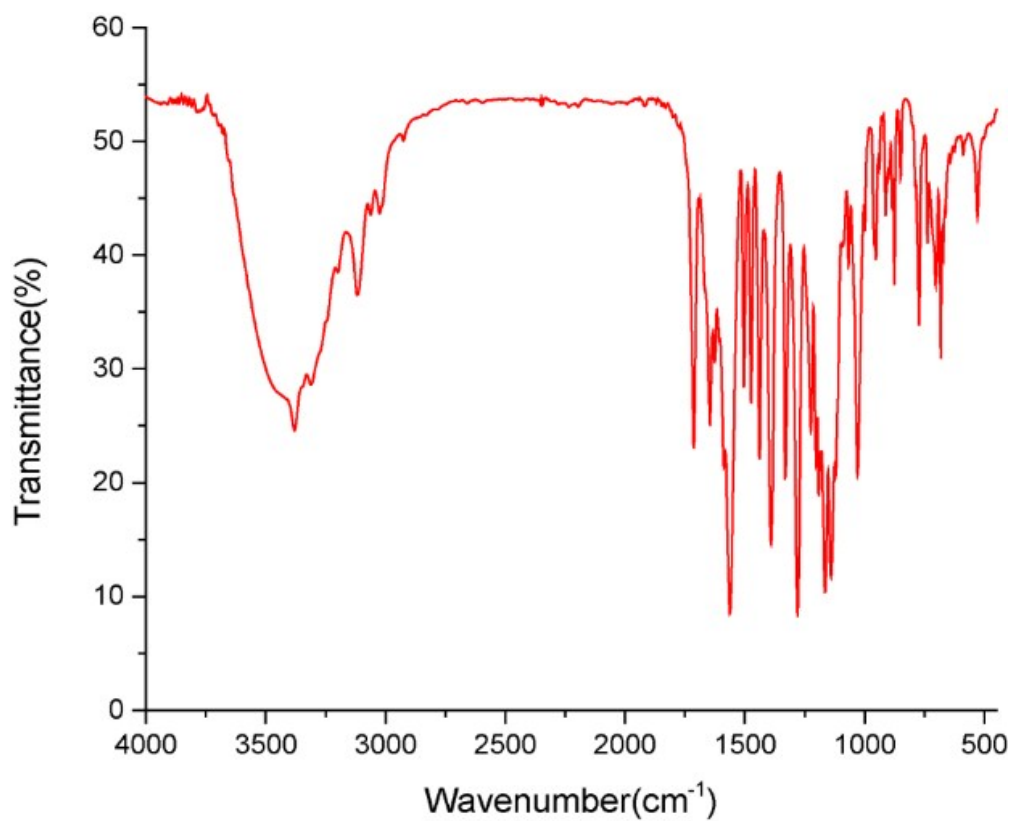


Figure S21: FT-IR spectrum of receptor **L₄** recorded in KBr pellet.

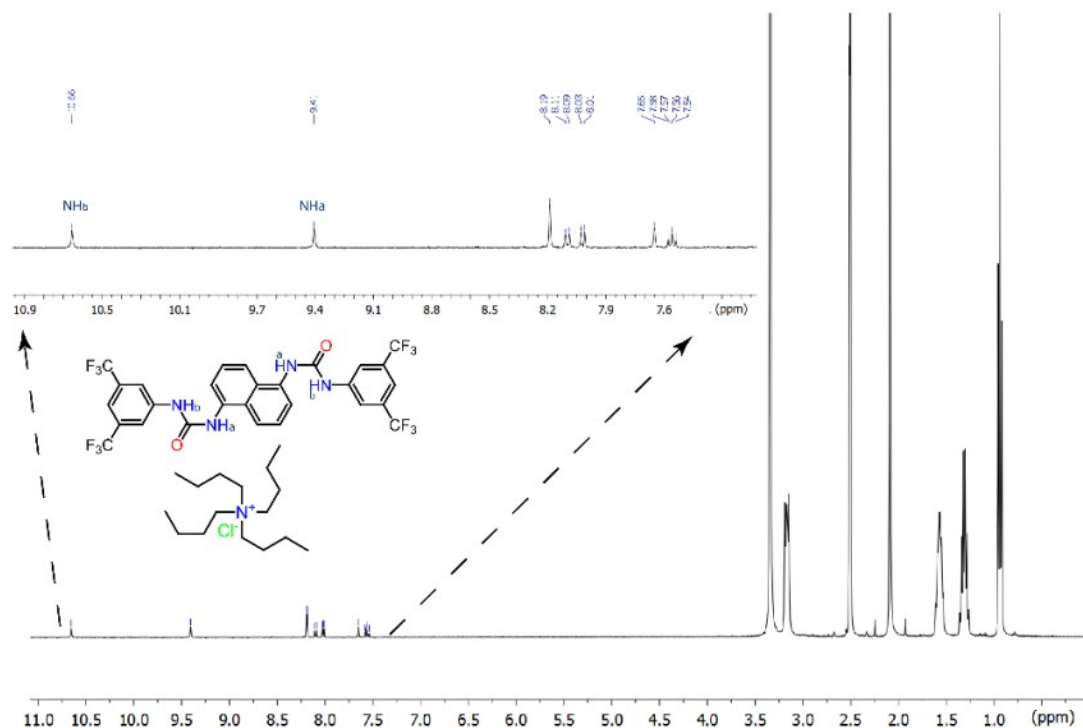


Figure S22: Integrated ^1H -NMR spectrum (full as well as expanded) and explanation of all hydrogen atoms of Chloride complex of receptor L_4 in DMSO-d_6 at 25°C .

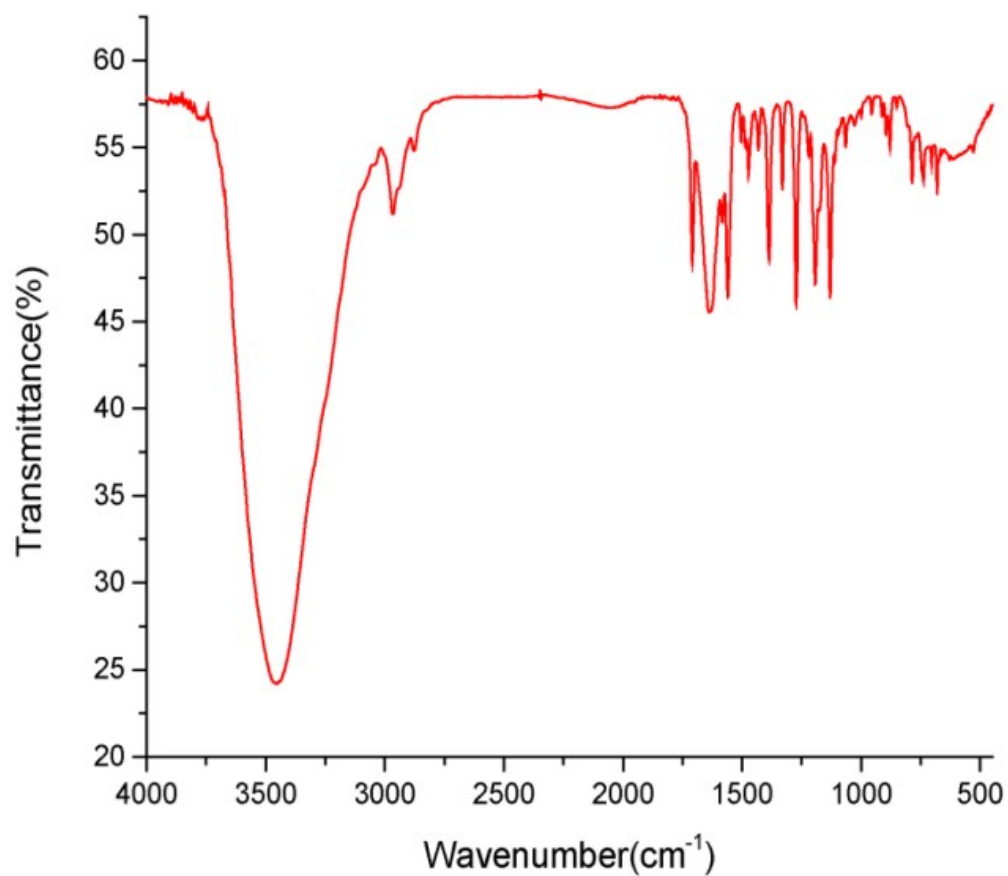


Figure S23: FT-IR spectrum of Bhl chloride complex of receptor L_4 recorded in KBr pellet.

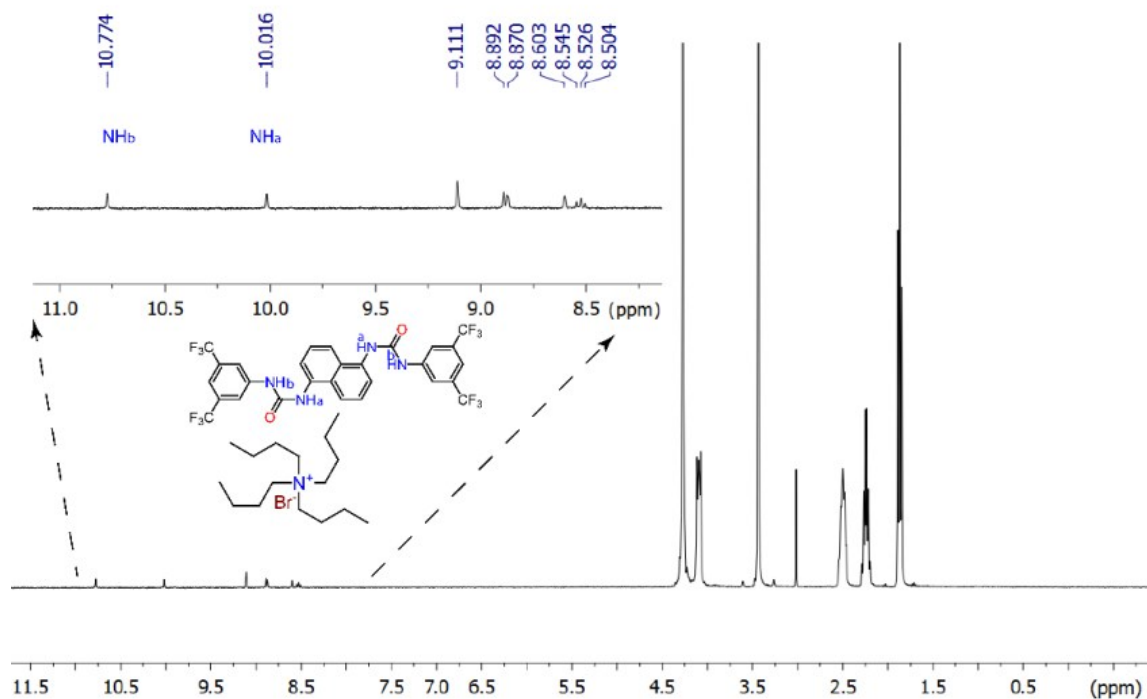


Figure S24: Integrated ^1H -NMR spectrum (full as well as expanded) Bromide complex of receptor L_4 in DMSO-d_6 at 25°C .

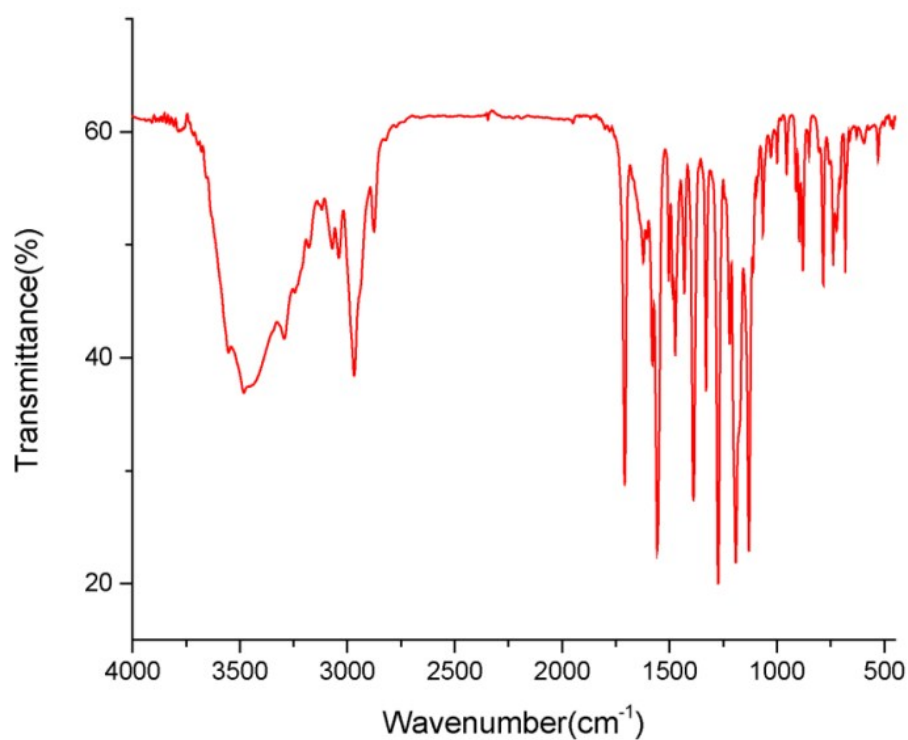


Figure S25: FT-IR spectrum of Bromide complex of dipodal receptor L_4 recorded in KBr pellet.

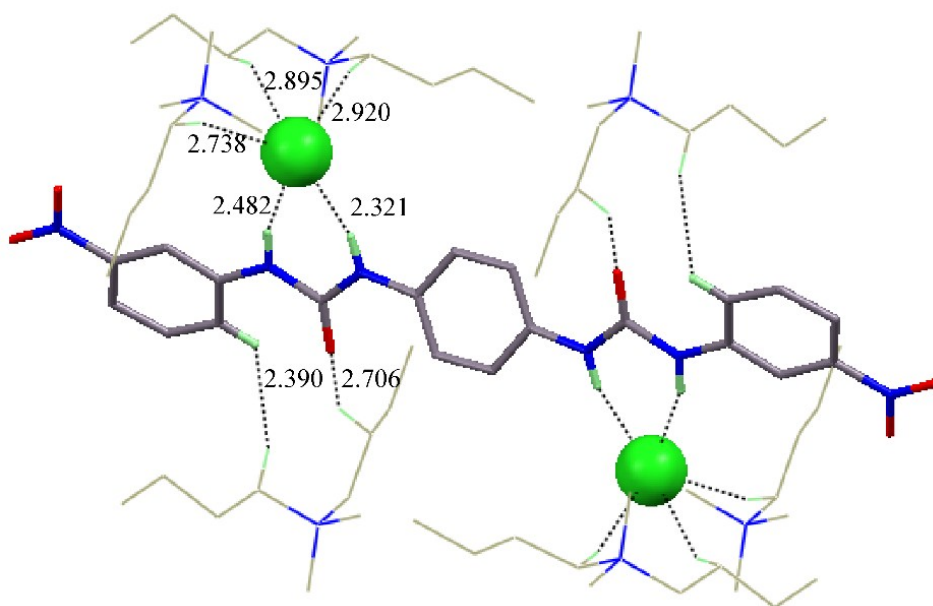


Figure S26: X-ray structure analysis of complex **1a** showing coordination environment of anion as well as extra stabilization through $\text{C-H}_{\text{aliphatic}} \cdots \text{O}_{\text{urea}}$ and $\text{C-H}_{\text{aliphatic}} \cdots \pi_{\text{aromatic}}$ interaction with proper bond distances in Angstrom.

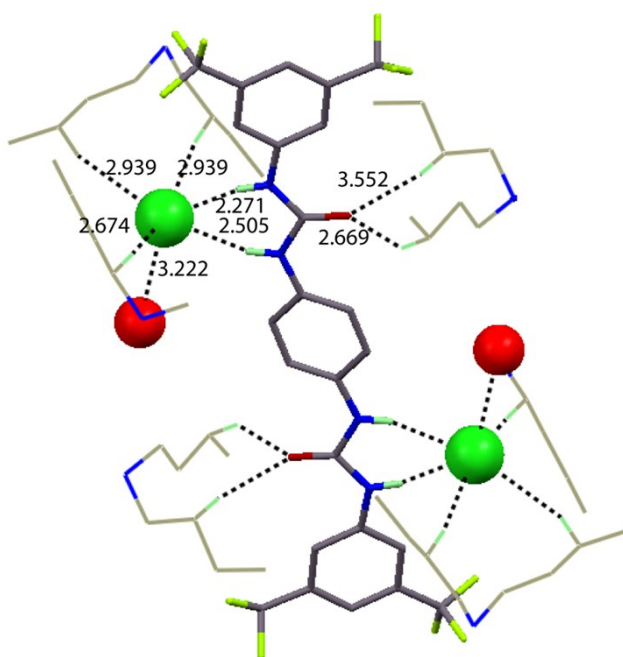


Figure S27: X-ray structure analysis of complex **2a** showing coordination environment of anion as well as extra stabilization through two $\text{C-H}_{\text{aliphatic}} \cdots \text{O}_{\text{urea}}$ with proper bond distances in Angstrom.

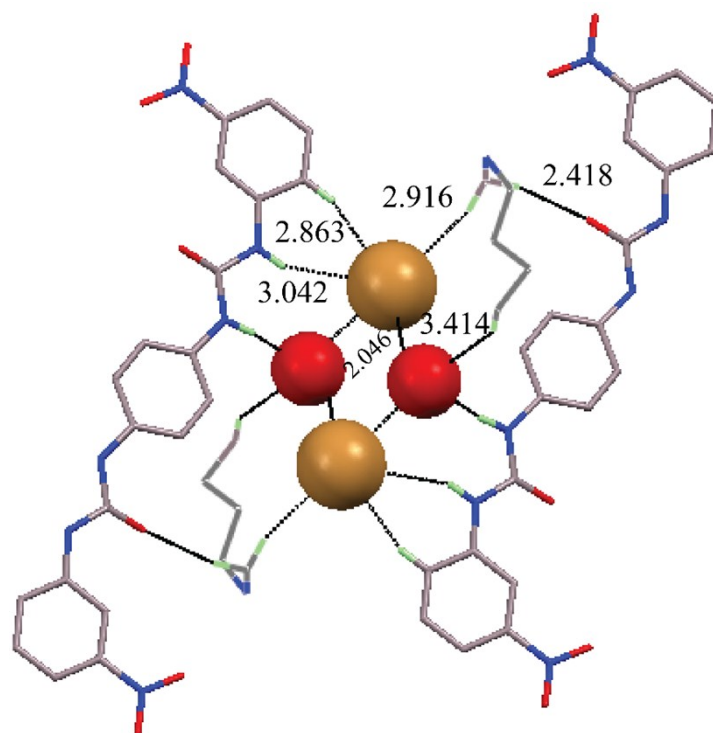


Figure S28: X-ray structure analysis of complex **1b** showing coordination environment of anion as well as extra stabilization through C-H_{aliphatic}...O_{urea}, C-H_{aliphatic}... π _{aromatic} C-H_{aliphatic}...O_{water} interaction with proper bond distances in Angstrom.

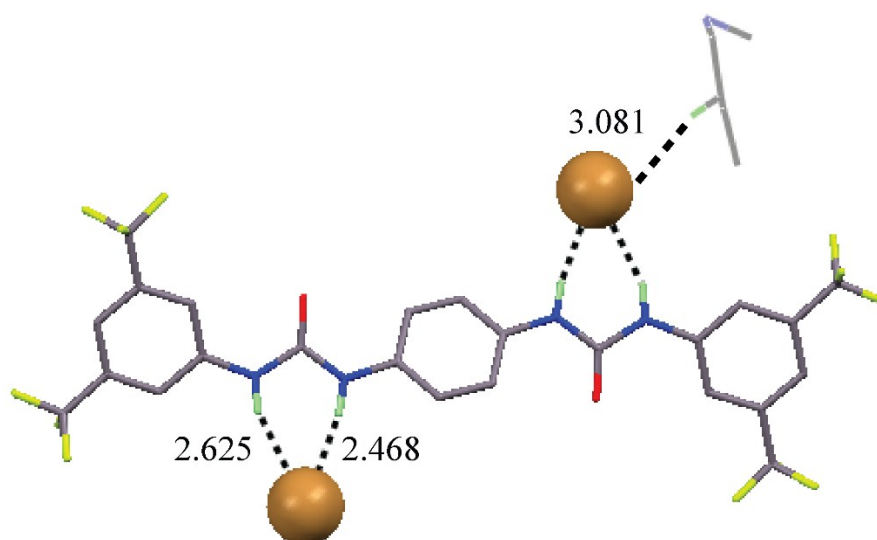


Figure S29: X-ray structure analysis of complex **2b** showing coordination environment of anion as well as extra stabilization through C-H_{aliphatic}...O_{urea}, with proper bond distances in Angstrom.

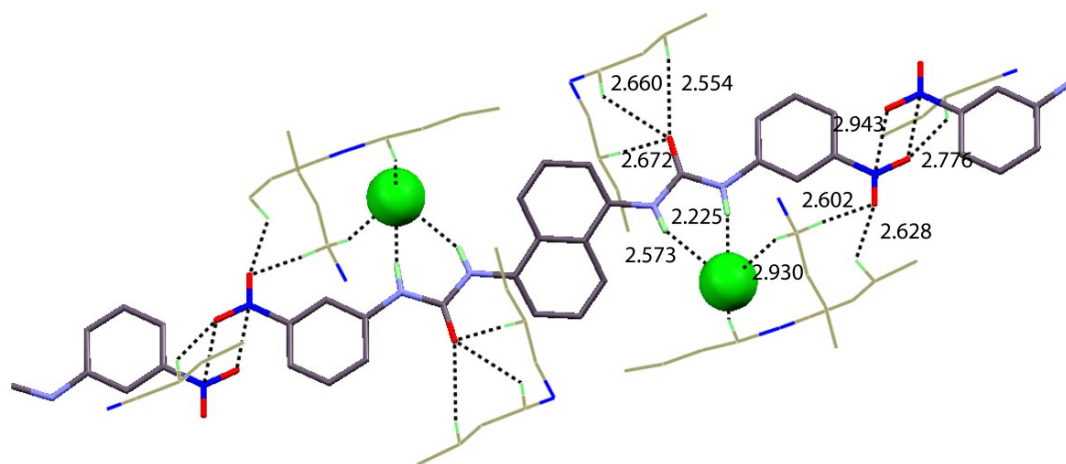


Figure S30: X-ray structure analysis of complex **3a** showing coordination environment of anion as well as extra stabilization through three C-H_{aliphatic}...O_{urea}, four C-H_{aliphatic}...O interaction from two different oxygen of substituted NO₂ group and one cross connected parallel C-H...O interaction between two NO₂ groups of each host site with proper bond distances in Angstrom.

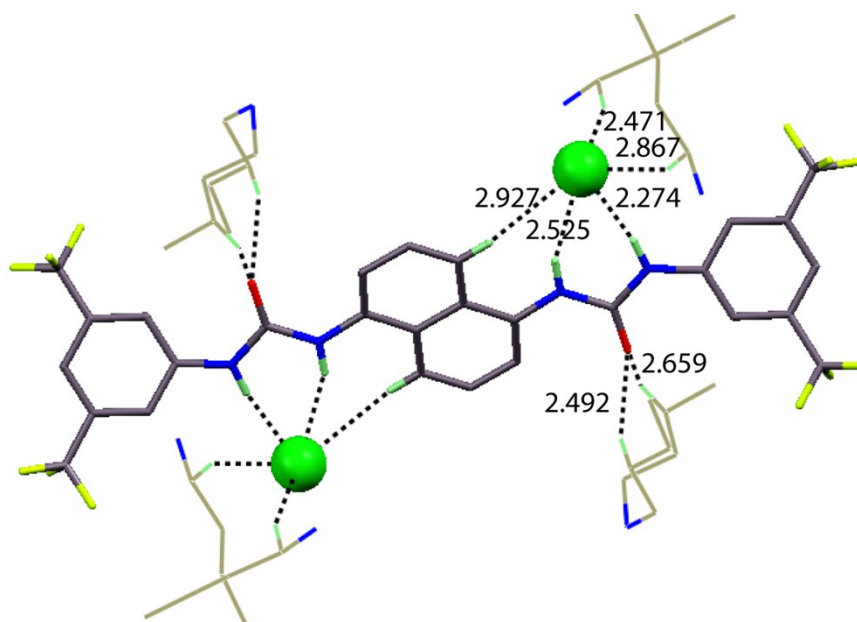


Figure S31: X-ray structure analysis of complex **4a** showing coordination environment of anion as well as extra stabilization through two C-H_{aliphatic}...O_{urea} interaction with proper distances in Angstrom.

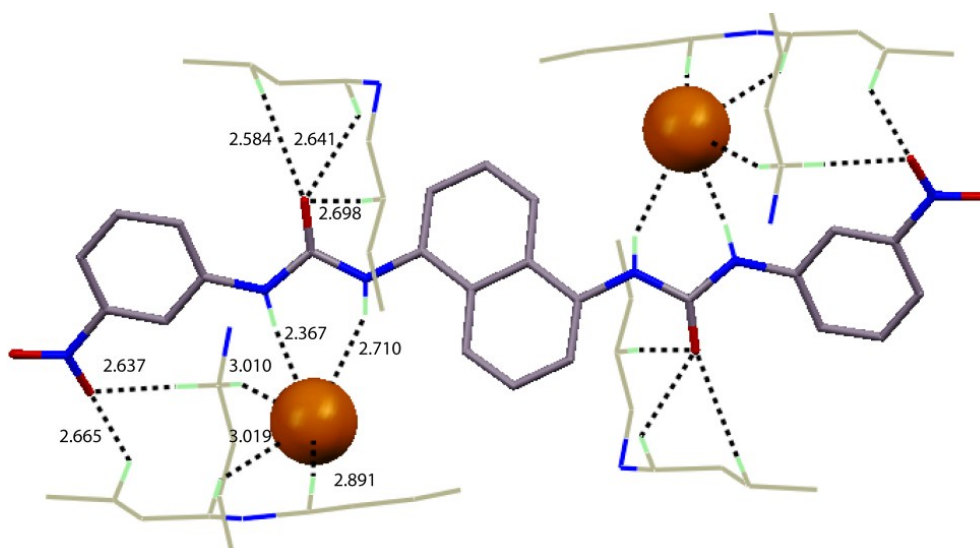


Figure S32: X-ray structure analysis of complex **3b** showing coordination environment of anion as well as extra stabilization through three C-H_{aliphatic}...O_{urea}, two C-H_{aliphatic}...O interaction involving one oxygen atom of substituted NO₂ group with proper bond distances in Angstrom.

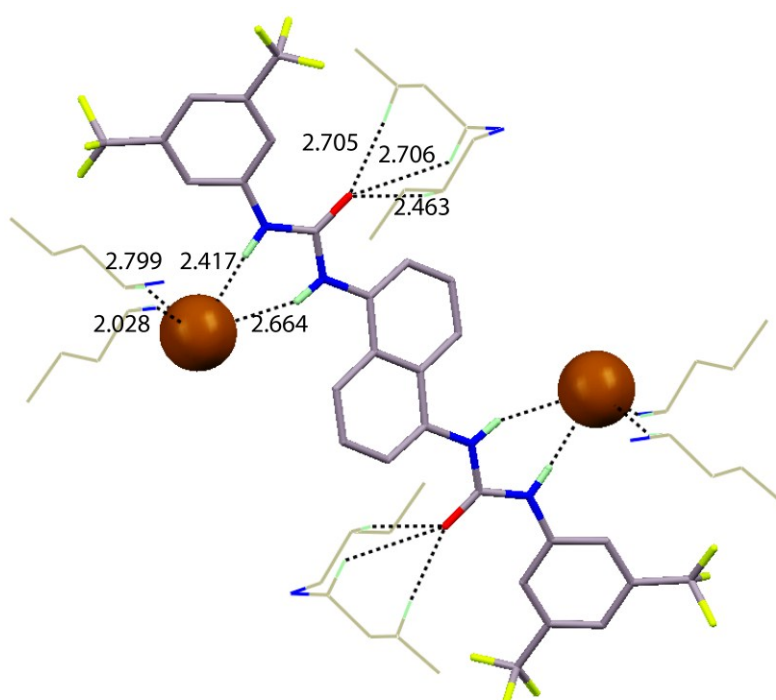


Figure S33: X-ray structure analysis of complex **4b** showing coordination environment of anion as well as extra stabilization through three C-H_{aliphatic}...O_{urea} interaction with proper distances in Angstrom.

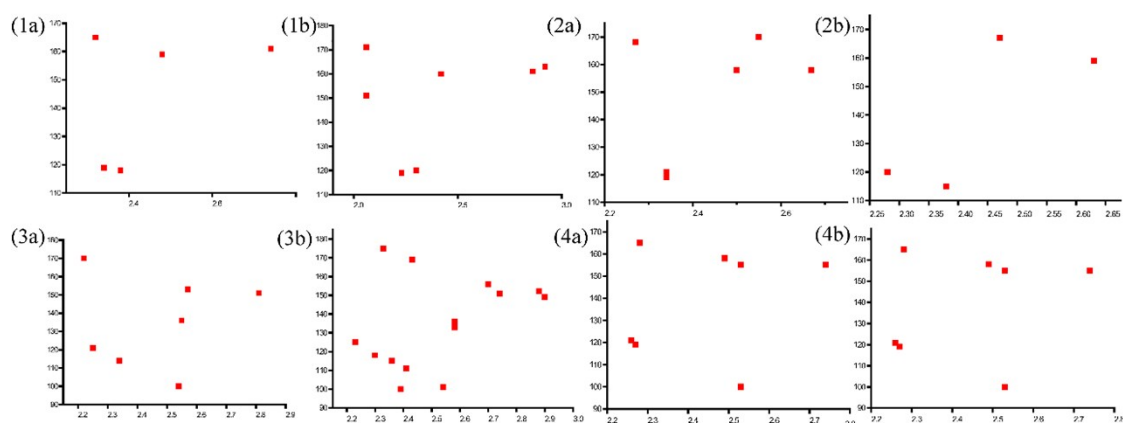


Figure S34: The scatter plot of N–H···A angle vs. H···A distance of the hydrogen bonds in the complexes (**1a**, **1b**, **2a**, **2b**, **3a**, **3b**, **4a** and **4b**).

Anion binding analysis by ^1H -NMR titrations — The ^1H NMR titration of the compounds was performed in $\text{DMSO-}d_6$ solvent. The stock solutions of the compound (10 mM), tetrabutyl ammonium Chloride (TBACl; 2 M) and tetrabutyl ammonium Bromide (TBABr; 2 M) were prepared in $\text{DMSO-}d_6$. The TBACl and TBABr were used as the source of Cl^- and Br^- ion. The changes in chemical shift ($\Delta\delta$) value of the N-H protons of the urea-moieties were analysed. Significant extents of chemical shift ($\Delta\delta$) of both N-H protons were observed. All ^1H NMR spectra were stacked through the MestReNova software. Changes in chemical shift against the concentration of Cl^- as well as Br^- ions were fitted using BindFit v0.5 program.¹

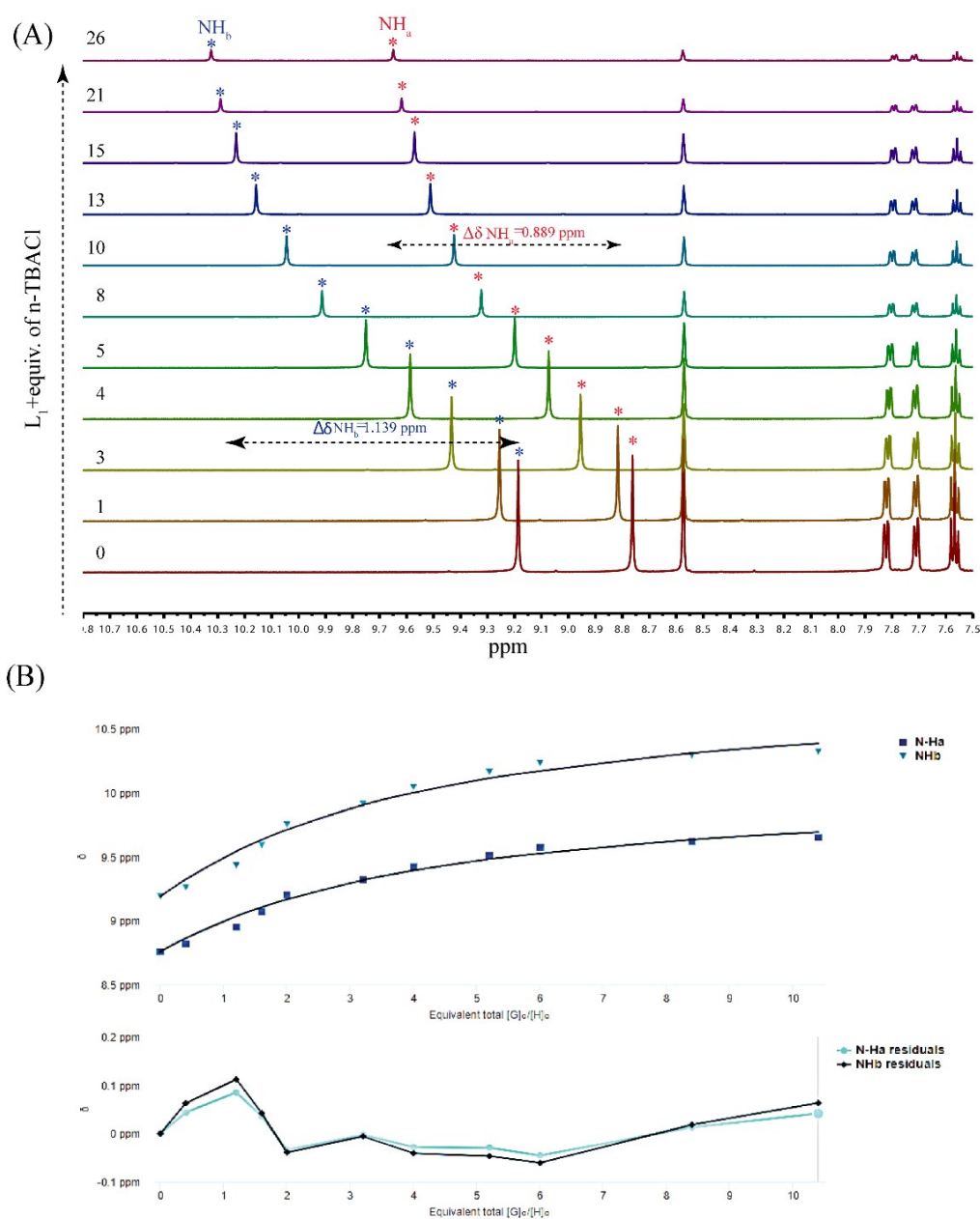


Figure S35: (A) Expanded partial ^1H NMR spectra of L_1 upon titration with $n\text{-TBACl}$ in DMSO-d_6 . (B) Showing the raw vs. fitted data (fitted to 1:1 NMR binding data) (top) and the corresponding residual plot (bottom). Binding constant (K) = 24.36 M^{-1} (Ref. 2).

(<http://app.supramolecular.org/bindfit/view/a04aa7b4-1b10-4ec4-b62a-004488bc153d>)

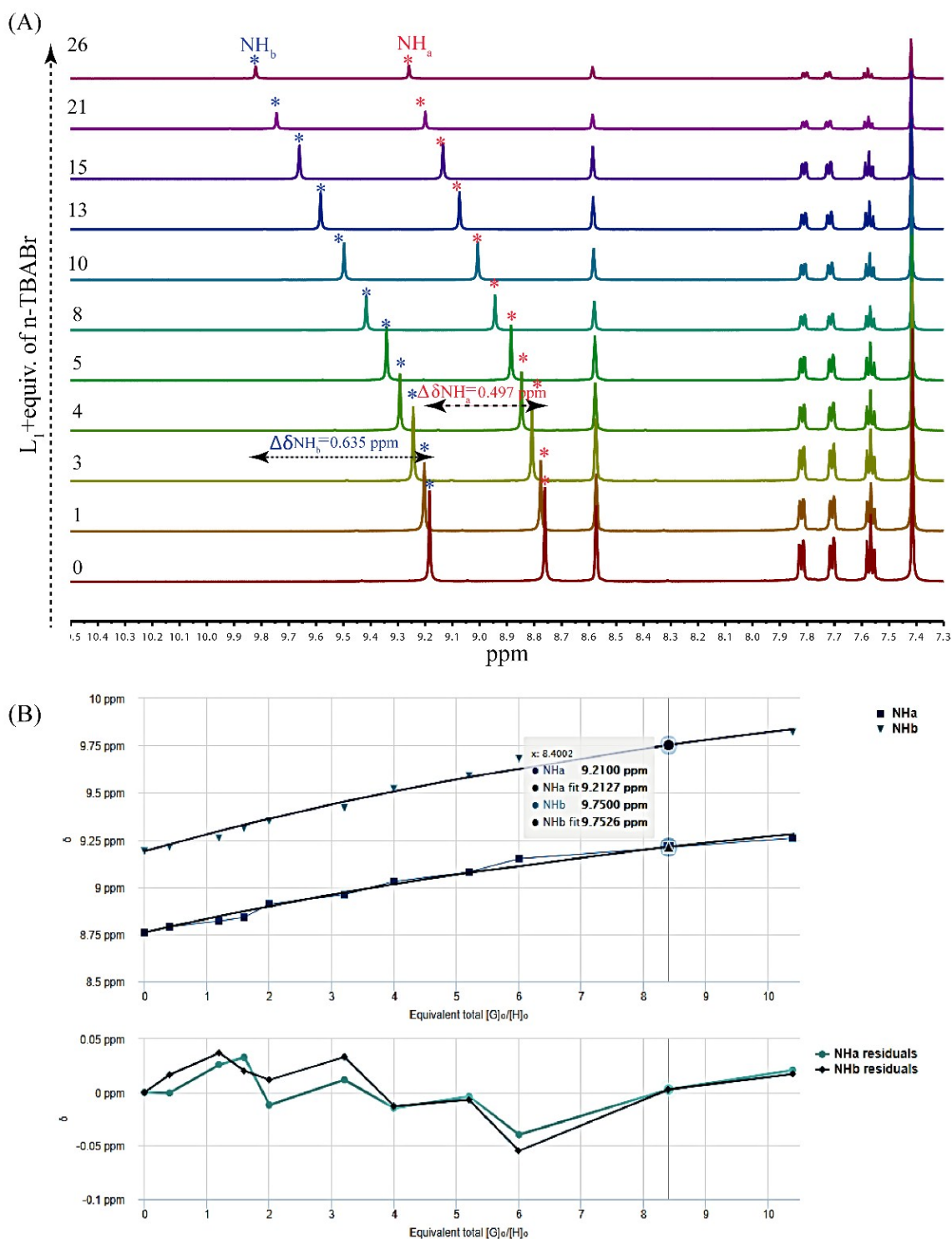


Figure S36: (A) Expanded partial ^1H NMR spectra of L_1 upon titration with n-TBABr in DMSO-d_6 . (B) Showing the raw vs. fitted data (fitted to 1:1 NMR binding data) (top) and the corresponding residual plot (bottom). Binding constant (K) = 2.85 M^{-1} (Ref 2).

(<http://app.supramolecular.org/bindfit/view/2f704e70-704c-4c4a-b586-861ec75747dc>)

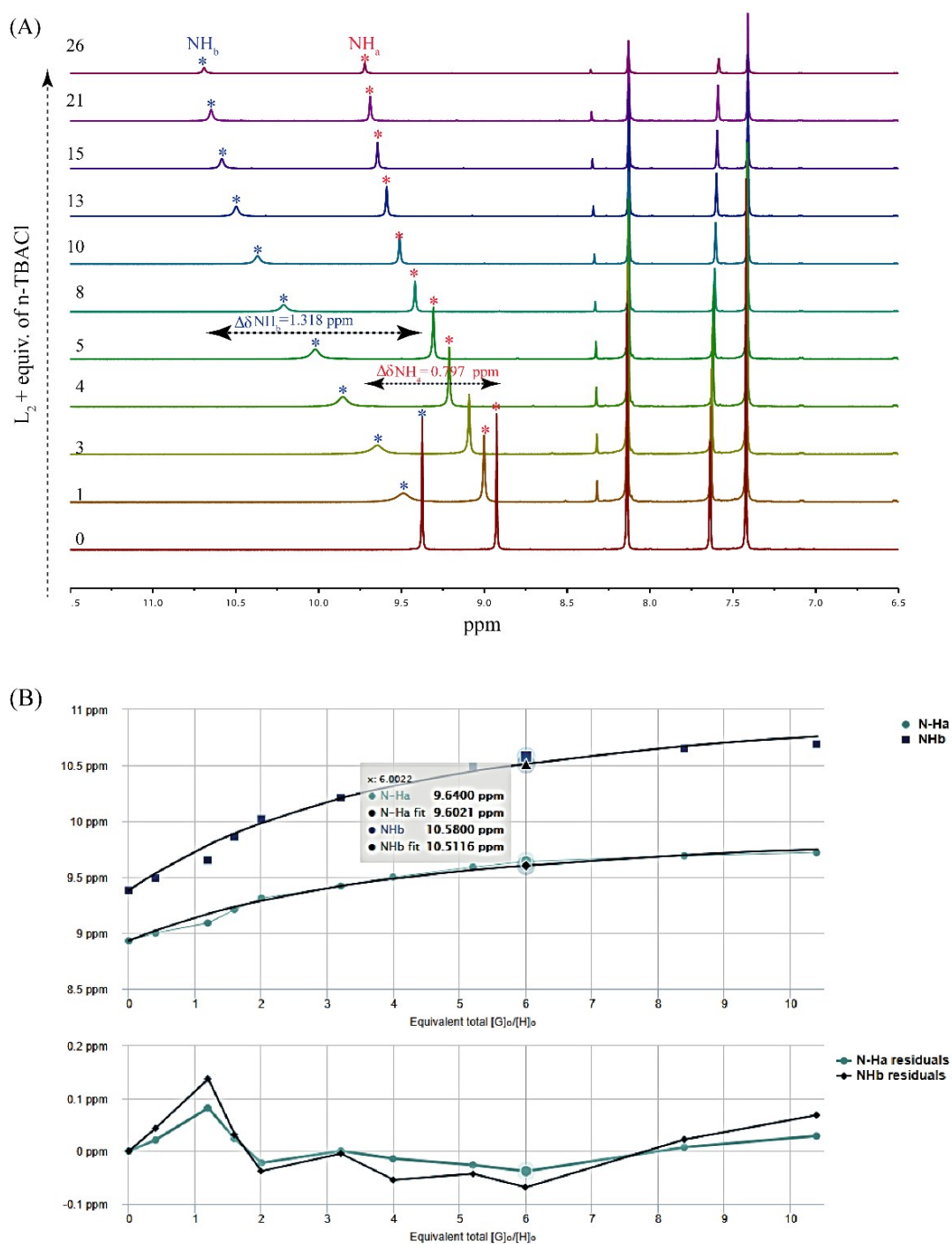


Figure S37: (A) Expanded partial ^1H NMR spectra of L_2 upon titration with $n\text{-TBACl}$ in DMSO-d_6 . (B) Showing the raw vs. fitted data (fitted to 1:1 NMR binding data) (top) and the corresponding residual plot (bottom). Binding constant (K) = 24.43 M^{-1} (Ref 2).

(<http://app.supramolecular.org/bindfit/view/ee741007-4a26-4279-9860-6c57eaca46fb>)

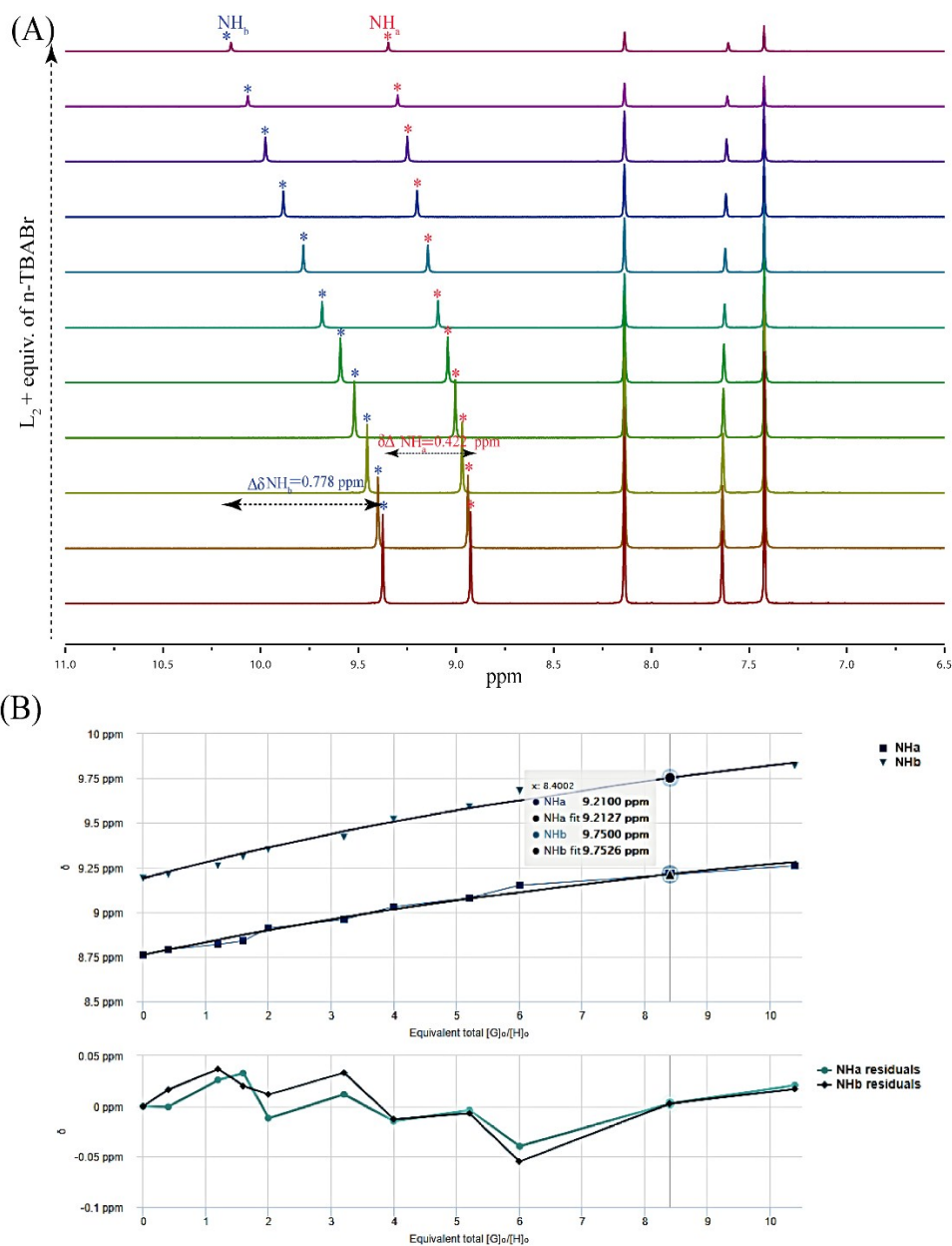


Figure S38: (A) Expanded partial ^1H NMR spectra of L_2 upon titration with n-TBABr in DMSO-d_6 . (B) Showing the raw vs. fitted data (fitted to 1:1 NMR binding data) (top) and the corresponding residual plot (bottom). Binding constant (K) = 2.72 M^{-1} (Ref 2)

(<http://app.supramolecular.org/bindfit/view/c24e85bf-7407-49e2-87cb-19270479e6fd>)

Table S1: Hydrogen bonding distances (Å) and Bond angles (°) in the neutral anion-receptor complexes:

Complex	D-H...A	d(D...H)/Å	d(H...A)/Å	d(D...A)/Å	<D-H...A/°	Symmetry codes
1a	N2-H2N...Cl1	0.86	2.48	3.299(5)	159	1-x, 1/2+y, 1/2-z
	N3-H3N...Cl1	0.86	2.32	3.159(5)	165	1-x, 1/2+y, 1/2-z
	C6-H6...O3	0.93	2.34	2.901(9)	119	x, y, z
	C10-H10...O3	0.93	2.38	2.934(9)	118	x, y, z
	C16-H16B...O1	0.97	2.61	3.515(1)	154	x, y, z
	C15-H15A...Cl1	0.97	2.92	3.861(7)	163	x, y, z
	C11-H11A...Cl1	0.97	2.74	3.669(7)	161	x, y, z
	C20-H20B...Cl1	0.97	2.89	3.748(8)	147	x, y, z
1b	N2-H2N...Br1	0.86	2.06	3.838(6)	151	-x, 1-y, -z
	N3-H3N...O4	0.86	2.05	2.898(8)	170	1-x, 1-y, -z
	C4-H4...Br1	0.93	2.86	3.753(8)	161	x, y, z
	C6-H6...O3	0.93	2.23	2.798(8)	119	x, y, z
	C10-H10...O3	0.93	2.29	2.867(9)	119	x, y, z
	C18-H18A...O3	0.97	2.42	3.348(10)	161	x, -1+y, z
	O4-H4A...Br1	0.85	2.70	3.413(7)	143	x, y, z
	O4-H4B...Br1	0.85	2.37	3.206(6)	167	1-x, 1-y, -z
	C18-H18B...Br1	0.97	2.92	3.851(10)	162	x, y, z
2a	N1-H1...Cl1	0.86	2.27	3.115(6)	168	x, y, z
	N2-H2...Cl1	0.86	2.50	3.317(6)	158	x, y, z
	C8-H8...O1	0.93	2.34	2.908(7)	119	x, y, z
	C12-H12...O1	0.93	2.34	2.929(7)	121	x, y, z
	C14-H14B...O1	0.97	2.55	3.510(8)	170	x, 1-y, 1/2+z
	C24-H24A...Cl1	0.97	2.67	3.589(6)	158	x, y, z
2b	N1-H1N...Br1	0.86	2.63	3.441(4)	159	x, y, z
	N2-H2N...Br1	0.86	2.47	3.312(4)	167	x, y, z
	C6-H6...O1	0.93	2.28	2.855(6)	120	x, y, z
	C11-H11...O1	0.93	2.38	2.894(6)	115	x, y, z
3a	N1-H1N...Cl1	0.86	2.57	3.360(2)	153	x, y, z
	N2-H2N...Cl1	0.86	2.22	3.076(2)	170	x, y, z
	C4-H4...O1	0.93	2.25	2.850(3)	121	x, y, z
	C9-H9...O1	0.93	2.34	2.854(3)	114	x, y, z
	C11-H11...N1	0.93	2.54	2.850(3)	100	1-x, 1-y, 1-z
	C14-H14A...O1	0.97	2.55	3.318(4)	136	x, y, z
	C20-H20B...Cl1	0.97	2.81	3.691(4)	152	x, -1+y, z
	N2-H2N...Br1	0.86	2.36	2.367(4)	173	1+x, 1+y, z

3b	N3-H3N... Br1	0.86	2.70	2.709(5)	154	1+x,1+y,z
	C16-H16...Br1	0.97	2.89	3.767(3)	150	1+x, y, z
	C22-H22B...O3	0.97	2.58	2.584(2)	134	x, y, z
	C22-H22A...O2	0.97	2.66	3.334(5)	126	x, y, z
	C23-H23A...O1	0.97	2.66	3.534(3)	149	x, y, z
	C24-H24A...O3	0.97	2.64	3.394(4)	134	x, y, z
	C27-H27A...O3	0.97	2.69	3.666(4)	175	x, y, z
	C28-H28A...O2	0.97	2.63	3.522(4)	151	x, y, z
4a	N1-H1N...Cl1	0.86	2.28	3.115(4)	165	x,y,z
	N2-H2N...Cl1	0.86	2.53	3.326(4)	155	x,y,z
	C7-H7...O1	0.93	2.27	2.835(6)	119	x,y,z
	C11-H11...O1	0.93	2.26	2.852(6)	121	x,y,z
	C13-H13...N2	0.93	2.53	2.841(5)	100	-x,1-y,-z
	C17-H17A...O1	0.97	2.49	3.414(6)	158	x,1-y,1/2+z
	C22-H22B...Cl1	0.97	2.74	3.642(5)	155	x,y,z
4b	N10-H10N...Br1	0.86	2.67	3.472(4)	157	x,y,z
	N17-H17N...Br1	0.86	2.42	3.258(4)	166	x,y,z
	C5-H5...O25	0.93	2.29	2.856(7)	119	x,y,z
	C24-H24...O25	0.93	2.26	2.851(8)	121	x,y,z
	C28-H28B...O25	0.97	2.47	3.390(9)	159	x,1-y,1/2+z
	C29-H29A...Br(1)	0.97	2.93	3.803(6)	151	x,1+y,z
	C35-H35A...Br(1)	0.97	2.80	3.702(6)	155	x,y,z
	C57-H57...N10	0.93	2.53	2.841(7)	100	x,y,z

Table S2: Contact contributions from the d_{norm} surface areas of dipodal segments in free receptors and in anion complexes.

Bond	1a	1b	2a	2b	3a	3b	4a	4b
C...H	21.4	16.9	11.8	9.5	20.3	19.9	15.2	14.7
O...H	19.6	27.6	10.5	3.4	20.5	20.3	11.6	11.8
F...H	0	0	24.8	36.4	0	0	24.6	24
N...H	4	4.6	2.4	1.7	3.9	3.9	2.4	2.4
H...H	37.8	33.6	21.4	22.3	41.2	41.2	25.1	25
Cl...H	12.7	0	19.2	0	11.2	0	8.5	0
Br...H	0	13.4	0	12.7	0	12.4	0	9.3

References:

1. D. Brynn Hibbert and P. Thordarson, Chem Commun, 2016, **52**, 12792-12805.
2. <http://supramolecular.org>.